Testing the expression and function of reformatted dimeric IgA to specifically target renal cyst luminal proteins.

MASTER'S THESIS

In partial fulfilment of the requirements for the degree

„Master of Science in Engineering "

Master Program:

"Biotechnology"

Management Center Innsbruck

Supervisor:

Dr. Thomas Weimbs (Professor)

Internal supervisor:

Dr. Carmen Nußbaumer (Professor)

Author:

Ilan Henzler (2010352031)

Preclusion from public access

I have requested preclusion from public access for this bachelor thesis until 10/02/2028, which was approved by the study program.

Innsbruck, Austria; 10/02/2023 _____

Declaration in lieu of oath

I hereby declare, under oath, that this master thesis has been my independent work and has not been aided by any prohibited means. I declare, to the best of my knowledge and belief, that all passages are taken from published and unpublished sources or documents have been reproduced whether as original, slightly changed, or in thought, and have been mentioned as such at the corresponding places of the thesis, by citation, where the extent of the original quotes is indicated. The paper has not been submitted for evaluation to another examination authority or has been published in this form or another.

Innsbruck, Austria; 10/02/2023 _____

Acknowledgements

This study was supported by a number of researchers, academics, and institutions which the author would like to acknowledge and express gratitude hereby.

Professor Weimbs of the University of California Santa Barbara hosted the project as principal investigator by granting access to the laboratory in which the experiments were conducted. His guidance shaped experimental procedures and interpretation. Ms. Schimmel, a PhD candidate at the Weimbs Lab, supervised laboratory work and offered guidance for experimental planning. Her in-depth understanding of dimeric IgA production processes was paramount for the successful completion of experiments. The author would also like to thank all other members of the Weimbs lab for their interest and support in the laboratory throughout the summer and fall terms of 2022.

Professor Nußbaumer of the Management Center Innsbruck agreed to become the internal supervisor for this thesis. Her academic lectures on the theory of immunology and drug development shaped the approach taken in this study. Her guidance during experimentation and thesis writing provided critical feedback and a sense of direction. Professor Griesbeck kindly established a connection to the University of California Santa Barbara, where this study was undertaken.

The author would also like to thank their home institution, Management Center Innsbruck, for initiating and fostering the academic exchange and the host institution, University of California Santa Barbara, for welcoming a visiting scholar and offering logistic support. This exchange would not have been possible without the Marshall Plan Foundation that created the opportunity for students to write their thesis at an institution in the USA and granted adequate financial support.

Sincere gratitude is due to the authors' family and friends for their ongoing interest and compassion.

Abstract

Autosomal dominant polycystic kidney disease (ADPKD) is the most common genetic kidney disease, affecting 12 million people worldwide. It manifests by the formation of cysts in the tubular lumen of kidney epithelial cells, leading to renal failure in half of all patients. The only FDA approved treatment option, Tolvaptan, slows cyst progression marginally but is associated with severe side-effects such as nausea, dehydration, and hypovolemia. One alternative is the development of monoclonal antibodies which can target disease-related proteins specifically, thereby minimizing side effects.

Of the five different classes of antibodies present in humans, only immunoglobulin A (IgA) has shown therapeutic potential to treat ADPKD through studies in the Weimbs Lab. The capacity for IgA molecules to form dimers allows them to target cyst-enclosed proteins by binding polymeric immunoglobulin receptor (pIgR). IgA has been shown to accumulate inside cysts and inhibit disease-related pathways. Following this discovery, studies have focused on optimizing IgA production and pharmacological properties to prepare preclinical models and render therapy feasible. These have highlighted the complexity of expression and characterization due to their polymeric conformation and heterogenous glycosylation.

This study focused on the optimization of dIgA expression via media supplementation and the characterization of dIgA function via binding assays. Dimeric IgA antibodies targeting IL13 cytokine were produced by transient transfection of HEK293-F cells followed by nickel chromatography and FPLC purification. Results indicate that batch supplementation with 1% Tryptone N1 reduces cell death post transfection and improves dIgA expression. The ability of dIgA to bind the pIgR was tested using transwells coated with Mandin Darby Canine Kidney (MDCK) cells stably expressing pIgR. Results validated dIgA binding to pIgR and transcytosis occurring with pIgR secretory component. This study established a modified setup of this assay which can verify dIgA transcytocis after 2,5 hours with fewer reagents.

The developed expression and characterization methods provide the potential for dIgA to be produced more efficiently and target proteins inside of pIgR expressing cysts.

Table of Contents

1. Introduction

Polycystic kidney disease (PKD) is the most common hereditary renal disorder worldwide. The autosomal-dominant type (ADPKD) is the most prevalent form, as one mutated allele inherited from a parent is sufficient to trigger disease progression. Similarly to tumors, PKD occurs due to excessive cell growth, in this case of renal tubule epithelial cells. This proliferation eventually leads to the formation of cysts which are fluid-filled, enclosed spaces lined by epithelial cells in the kidney. Since cyst growth is promoted through an internal feedback loop, they continue to grow, leading to renal failure in roughly half of all patients. ADPKD affects all genders and ethnic groups and globally over 12 million people. Current estimations postulate the incidence to be 1 in 400 to 1 in 2500 people. While people with early ADPKD can reduce their symptoms by adjusting their diet and lifestyle, patients at later stages may require haemodialysis and kidney transplants [2].

The only medicine approved to treat ADPKD, called Tolvaptan, has been shown to slow cyst growth and improve patients' kidney function by 6% after 5 years of treatment [3]. It is however associated with severe side effects such as dehydration, hypovolemia, and liver injury due to its systemic effects on vasopressin receptor in other body parts [4]. Other therapy options treat disease symptoms such as pain and high blood pressure or suggest dietary changes such as a ketogenic and time-restricted dietary regimens [5]. The inability of small molecule (SM) drugs such as Tolvaptan to target disease-related proteins specifically, has also spurred an active area of research in biologics as alternative therapies. Antibodies are one such compound that bind their target exclusively, thereby reducing side-effects.

Commented [Ga1]: Zusammenhang fehlt

Commented [i2R1]: danke, so evtl. besser

Antibody therapeutics are developed exclusively using IgG isotypes due to their ability to recruit effector cells for antibody-dependent cellular cytotoxicity (ADCC) [6]. In the case of ADPKD where cysts form inside of the kidney lumen, IgG therapy is rendered ineffective as it cannot cross the epithelial cell layer to target cyst. Here, another isotype namely IgA has shown promise as its dimeric form can target cyst-enclosed proteins. This occurs through polymeric immunoglobulin receptors (pIgR) which recognize dimeric IgA (dIgA) and actively transport it across epithelial membranes to release it into cyst lumen. In light of this discovery, recombinant dIgA production methods have been improved to support their

therapeutic function and render small-scale rodent studies feasible [7]. The following study seeks to optimize recombinant dIgA expression and characterize its receptor-mediated transcytosis function in-vitro. In addition to ADPKD, other diseases would benefit from improved IgA production and characterization, as it would facilitate candidate testing.

2. Theoretical Basics

2.1. Polycystic Kidney Disease

2.1.1. Disease Profile

Polycystic kidney disease (PKD) is a subset of chronic kidney disease associated with the loss of kidney function because of the bilateral formation of cysts in renal tubular epithelia. There are two types of PKD based on allele frequency. The autosomal dominant (ADPKD) the more common version occurring in 1:400 to 1:1000 people [1] and the rarer paediatric autosomal recessive (ARPKD) version occurring in 1:20.000 people worldwide. While both diseases feature kidney enlargement, in ADPKD, cysts form in the nephron, with extra-renal presentations manifesting as liver and pancreatic cysts whilst in ARPKD cysts form in the collecting duct with extra-renal manifestations such as hepatic and biliary duct hyperplasia [8]. Figure 1 shows the structure of a human kidney nephron without PKD (A) and a patient suffering from ADPKD (B) where cysts form on renal epithelia [64]. Resulting cysts cause further damage such as infections and may eventually lead to renal failure.

Figure 1: Structure of a kidney nephron for normal adults and ADPKD patients

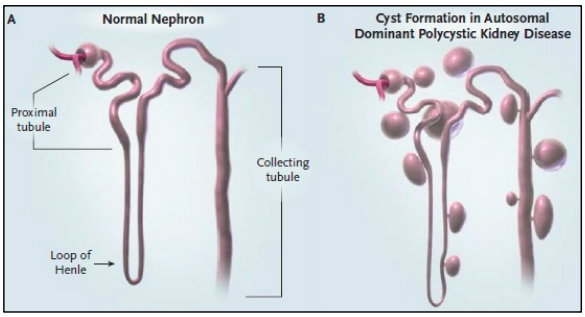

2.1.2. Genetic Basis

The onset of ADPKD is associated with mutations in either *PKD1* or *PKD2* genes with mutations in *PKD1* accounting for 80-85% of ADPKD cases [9]. These mutations lead to defects in proteins polycystin-1 (PC1) or polycystin-2 (PC2), respectively. PC1 is a 485 kDa protein found in lateral membranes of cell contact areas such as cellular junctions and

Commented [Ga3]: more detailed, size, location expression profile...

Commented [i4R3]: danke, zu expression profile ist nicht sehr viel bekannt doch ich könnte noch erweitern

desmosomes [10]. It has 11 transmembrane domains, a large extracellular and a short cytoplasmic C-terminal domain which forms a heterodimer with calcium-sensitive ion channel PC2 on primary cilia [11]. PC2 is a 130 kDa protein which localizes on the endoplasmic reticulum (ER), primary cilia and plasma membrane. In addition to its channel function, it acts as a regulator in intracellular signalling [12]. While the exact function of both proteins is still under investigation, some studies have shown that together, they build calcium-regulated ion channels on the cilia of renal epithelial cells [13]. This is supported by studies showing that a loss of polycystins is correlated with disruptions to flow dependent intracellular Ca^{2+} signalling [14]. In renal cilia, the PC1/PC2 complex seems to act as a mechanosensor, by converting extracellular mechanical stimulation to an intracellular biochemical response. This could explain why defects in PC1 & PC2 hamper the transduction of signals by movement-sensitive cilia, responsible for detecting fluid flow in renal tubules [15]. Since PC1 & PC2 co-localize to other cellular structures, it is unclear if the PKD phenotype is a result of cilia dysfunction alone. However, an apparent link exists between abnormal PC1/PC2 complex and excessive proliferation of renal tubule epithelial cells.

2.1.3. Protein Pathways Involved

Because of the involvement of PC1 & PC2 in many molecular pathways, studies have focused on the ones highly upregulated in ADPKD disease models. One of these is cyclic adenosine monophosphate (cAMP), triggered by reduced intracellular calcium levels and vasopressin 2 receptor (V2R) activation [16] [17]. This then drives cell proliferation via the ERK/MAPK pathway. When targeting V2R with an antagonist such as Tolvaptan, a reduction of cAMP levels and associated MAPK activation can be achieved, reducing cystogenesis [18]. Another important pathway in ADPKD pathogenesis is that of EGFR, which is activated following mislocalisation to apical membranes and contributes to cystogenesis in ADPKD rodent studies [19]. Treatment with epidermal growth factor receptor (EGFR) inhibitors however, worsened the cystic phenotype indicating that EFGR signalling may not be needed for cystogenesis [20]. Studies investigating ADPKD pathway interactions showed that cellular processes downstream of EGFR such as mitogen-activated protein kinase (MAPK), mammalian target of rapamycin (mTOR) and signal transducer and activator of transcription 3 (STAT3), are also highly activated, spurring studies to target these proteins [16] [21] [22].

2.2. Immunotherapy

2.2.1. Immunological Foundations

Humans have five antibody isotypes, distinguished by their constant regions. Immunoglobulin G (IgG) is the main form of circulatory immunoglobulin in the body and presents the longest half-life. In terms of overall quantity, more IgA is secreted in the body than all other isotypes combined [26]. One IgA antibody unit is made up of four polypeptide subunits: two identical heavy chains linked to two identical light chains by disulphide bonds. These are further subdivided into domains where the light chain consists of one variable V_L and one constant C_L domain while the heavy chain consists of on variable and three constant domains Cα connected via hinge regions (Figure 2 [65]). Structurally, antibodies can be partitioned into a constant, fragment crystallizing (Fc) and two variable, fragment antigen binding (Fab) regions, with the latter granting target-specificity. Most IgA is released into mucosal surfaces such as those of the respiratory system to provides immunologic protection against infectious airborne diseases like influenza, measles, and bacterial lipopolysaccharide [28]. After forming a complex with its antigen, IgA crosslinks its receptor, called FcαRI, on immune cells such as neutrophils, monocytes, and macrophage. This activates them and the resulting pro-inflammatory response includes antibody mediated cytotoxicity (ADCC), phagocytosis and release of cytokines which eliminate pathogens [29].

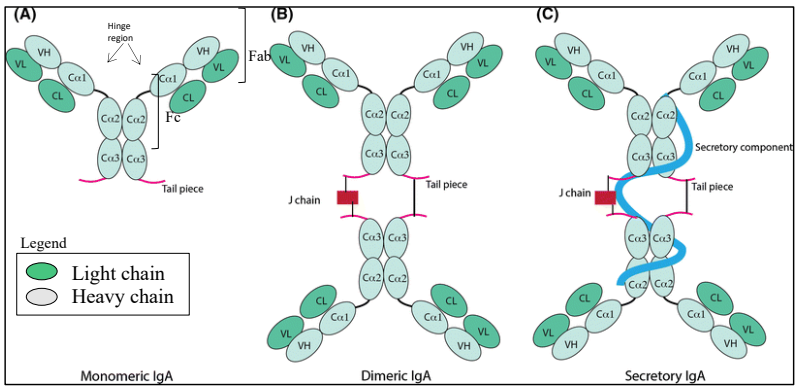

Figure 2: IgA in monomeric, dimeric and secretory component form

Commented [Ga5]: describe the figure in the figure text

Commented [Ga6]: ausschreiben

Commented [Ga7R6]: Beschreibung

Commented [i8R6]: Beschreibung des lipopolysaccharide?

All hominoid primates possess two IgA subclasses, IgA1 and IgA2 which differ in the size of their hinge region. While it constitutes 85% of total IgA in serum, IgA1's longer hinge in makes it vulnerable to proteolytic attack by pathogenic bacteria [36]. This could be why IgA2 predominates in mucosal secretions, with their differently constituted hinge regions also suggested to explain improved granulocyte recruiting abilities [37]. IgA antibodies are characterized by heavy and heterogenous glycosylations. IgA1 has two N-linked glycosylations in the heavy chain constant domain and multiple O-linked glycosylation sites in the hinge region. While IgA2 lacks O-linked glycans, it has four to five N-linked glycans [69]. Glycan heterogeneity is divided into micro- and macroheterogeneity where microheterogeneity refers to glycan variability and macroheterogeneity refers to glycan presence or absence at each glycosylation site. These heterogeneities can majorly impact solubility, serum half-life and ADCC. N-linked glycans of IgA antibodies have been shown to be essential for antiviral activity [33] [34]. In IgA2 for example, sialyation of the Cα1 region is required to perform cell-mediated reverse transcytocis for pathogen uptake [70]. Other IgA glycosylations have been linked to disease with aberrantly O-glycosylated IgA1 involved in the development of IgA nephropathy by forming immune complexes with IgG [35].

IgA molecules are able to exist in a dimeric form where two monomers (Figure 2A) are covalently bound by disulphide bridges between their tail pieces and a J-chain (Figure 2B) [38]. This dimeric IgA (dIgA) is synthesized by B cells in the lamina propria, located at the basolateral surface of mucosal epithelia. Due to its conformation dIgA can bind pIgR, a transmembrane protein found on the epithelial lining of mucosa and GI tract. Recognition of the J-chain by pIgR stimulates transcytocis of the receptor-bound dIgA via clathrin-coated pits through epithelial cells [71]. At the apical side of cells, a section of pIgR is cleaved and covalently attached to one of dimeric IgA's α chains as secretory component (sIgA) (Figure 2C). This complex is released into mucosal lumen, where secretory component protects dIgA from proteolytic cleavage. In the mucosal lumen, sIgA can then not only bind pathogens and elicit ADCC but also bind mannose-binding lectin to activate complement-dependent cytotoxicity [39]. The ability to bind pIgR and pass through epithelia is a key function of immunity as it also impedes intracellular viral replication and enables the exclusion of pathogens which have penetrated the lamina propria [71][29]. In kidneys, the pIgR/dIgA system can be naturally upregulated to protect the urinary space from pathogens [2].

Commented [Ga9]: this is figure 2

2.2.2. IgA as Immunotherapy

The potential of the IgA in immunotherapy is being investigated due to its potent target neutralization in-vivo and ability to exist in multiple oligomeric forms, to target proteins in a new and more effective manner (Kim 2017). With dIgA able to target pIgR and undergo transcytocis in natural immunity, an application to target markers in cyst lumen was studied. These efforts showed that intraperitoneally injected dIgA targets pIgR on cyst lining epithelial cells and undergoes transcytosis [2]. With renal cysts having lost their connection to the tubular system, dIgA is trapped in the cyst lumen and accumulates over time (

Commented [Ga10]: Introduction sentence why to use IgA for immuntherapy

Figure 3 [66]). Due to its short half-life, it is assumed that unbound IgA is secreted through the intestinal epithelium and bile, minimizing the risk for systemic side-effects [32] [41]. With dIgA's cyst targeting abilities validated, further studies looked for signalling molecules highly expressed in renal cyst-lining epithelial cells. Weimbs et. al identified transcription factor STAT6 as a potential therapeutic target in PKD and showed that its activation regulated by PC1, leads to cyst growth [23]. In cysts, STAT6 is activated by cytokine interleukin 13 (IL13) via IL4/IL13 receptor activation. With STAT6 activation also causing IL13 secretion into cyst fluid, it constitutes a positive feedback loop as secreted molecules cannot be cleared [24].

Commented [GU11]: Edited by MS (tracking off on accident)

With STAT6 established as a promising target for PKD, studies have shown that non-specific pharmacological inhibition using leflunomide and gene ablation of STAT6 could reduce renal cyst growth in PKD mice [40]. To overcome leflunomide's non-specificity and related side effects, specific inhibition of signalling pathways can be achieved by antagonistic antibodies against growth factors or their receptors. This suggests that dIgA could be used for STAT6 pathway inhibition and is supported by studies showing that in ADPKD mice models, STAT6 activation increases pIgR expression on cyst-lining cells [25] [2]. Considering the proteins involved in the STAT6 pathway, IL13 was chosen as a target for dIgA because of its feedback role. Anti-IL13 dIgA were engineered and their intraperitoneal injection in ADPKD mice models was shown to bind IL13 and inhibit STAT6 phosphorylation, reducing cyst growth in a dose-dependent manner [42] [24]. In summary, the applicability of dIgA in ADPKD therapy has shown promise in initial studies, setting the stage for validation and scaling production.

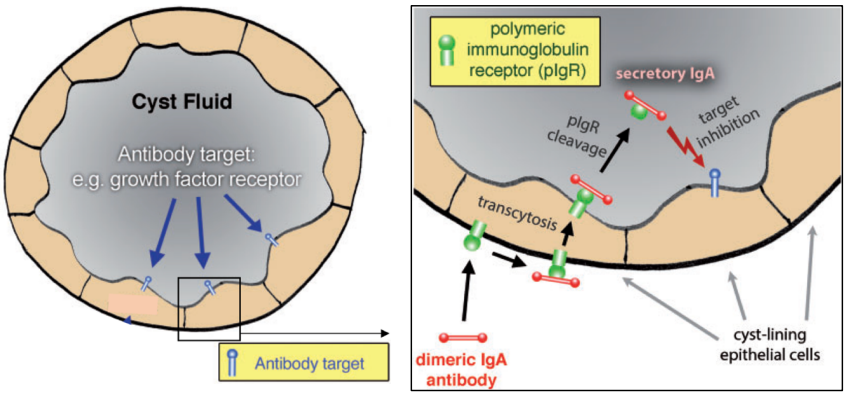

Figure 3: Schematic of dIgA pIgR binding and transcytocis

2.2.3. IgA Production

Challenges in IgA manufacture revolve around reproducing their complex structures in therapeutically relevant yields [43]. With heterogenous glycosylation patterns affecting expression and degradation pathways, ICH guidelines specify the control and characterization of mAb glycosylation profiles [72]. Methods to control glycosylations have been centred on cell-line engineering to yield predictably glycosylated mAbs [74] and media additives to manipulate metabolic pathways involved in glycan formation [Durocher, 2004]. Methods for glycoprofiling have employed analytical tools such as lectin-microarrays coupled with MS [Pazitna, 2020]. Mammalian cell lines such as CHO cells have been most prevalently used for IgA production since they can achieve glycosylation patterns similar to humans [44]. These could also minimize immunogenicity concerns by using serum-free expression media. This improved both the downstream process and the ability to adhere to quality requirements for use in-vivo. Following these developments, dIgA1 with therapeutically viable post-translational modifications could be produced with yields above 100µg/ml [45] [46]. Nevertheless, the development of optimal expression media still remains a challenge, due to its significant impact on process productivity and protein glycosylation (Li, 2009). Therefore, this study chose to focus on the media supplementation to improve dIgA titer and function.

3. Aim

The scope of this thesis includes the generation and characterization of dIgA, a dimeric antibody antagonistic to cytokine IL-13 involved in ADPKD. This includes the expression and purification of adequate yields as well as the in-vitro characterization of dIgA transcytocis properties. Accordingly, the content of this thesis can be divided into two parts.

The first part focuses on the optimization of existing protocols to produce IgA. The tasks were to generate purified plasmids, perform transient transfections and purify resulting dIgA from supernatant to therapeutic quality. Protocols were optimized by recording process changes and correlating them with output parameters. Given the need to investigate how changes in media supplementation could improve the viability and productivity of dIgA expression, trials were also designed to assess the effect of additives on cell growth and productivity. After a small scale study, selected batch conditions were scaled up along with fed-batch supplementation. In the final trial, the most promising condition was compared with standard transfection conditions.

The second part considers the structure of the generated dimeric IgA and its function in-vitro. In addition to validating the ability of generated antibodies to undergo transcytocis, a formulated goal was to consider which glycosylation patterns were present and how they may affect transcytocis. For this, tasks were focused on modifying glycosylation levels on purified dIgA using the PNGase enzyme and testing the binding function of aberrantly glycosylated dIgA using a transcytocis assay. In addition, subtle modifications to the original transcytocis setup were tested and consolidated into an improved version of the set-up.

Commented [Ga12]: do not use my

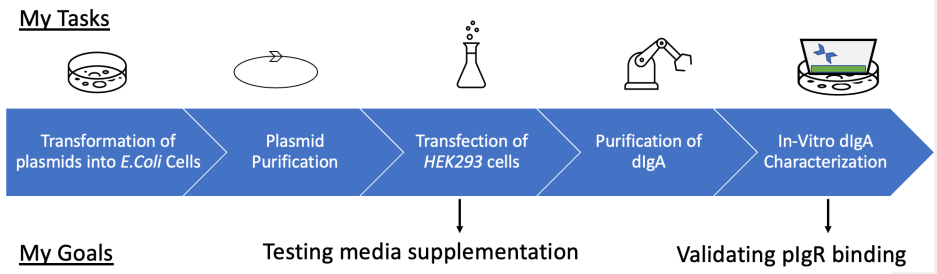

Figure 4: Workflow of recombinant dIgA production

4. Materials

4.1. Chemicals

Table 1: Chemicals used with name, purity, CAS number, manufacturer and category number

Chemical	Purity	CAS-No	Manufacturer	Cat-No
Ampicillin	≥99.0%	69-53-4	ThermoFisher	J60977.06
Blasticidin	≥99.0%	09.03.13	ThermoFisher	R21001
Bovine Serum Albumin	≥96%	9048-46-8	Sigma-Aldrich	A2153-100G
D-Mannose	≥99%	3458-28-4	Millipore-Sigma	M6020
D-PBS - Cl2H3K2Na3O8P2	≥99%	/	Cytiva	SH3002801
Dithiothreitol (DTT)	≥98%	03.12.83	Sigma-Aldrich	3870
DMSO - $(CH_3)_2SO$	≥99.5%	67-68-5	Fisher Scientific	BP231-100
Ethanol 70% - C_2-H_6O	≥99.5%	64-17-5	Lab Alley	EAP200
Galactose	≥99%	59-23-4	Millipore-Sigma	PHR1206
Glutamine	≥99%	56-85-9	Millipore-Sigma	1294808
Glycerol	≥99.5%	56-81-5	EMD	GX0185-6
Hydrogen Chloride - HCl	≥99%	7647-01-0	EMD	HX0603-4
Isopropanol – C_3H_8O	≥99.8%	67-63-0	Lab Alley	IPAL99
L-Asparagine	≥98%	70-47-3	Millipore-Sigma	A4159
Liquid Nitrogen - LN_2	≥99.998%	7727-37-9	Linde	P-4630
MassRuler™ DNA Ladder Mix	≥99.0%	2631252	ThermoFisher	SM0403
Methanol - CH_3OH	≥99.8%	67-56-1	EMD	MX0485P-4
PEI	≥99%	9002-98-6	Sigma-Aldrich	408727
Penicillin	≥99.5%	3810-74-0	ThermoFisher	15140122
Phenylmethylsulfonylfluoride (PMSF)	≥99%	329-98-6	EM Science	7110
Ponceau S	75%	6226-79-5	Biomedicals	151942
Protease inhibitor	MQ200	200-664-3	Sigma-Aldrich	P0044-1ML
Sodium Chloride - NaCl	≥99%	7647-14-5	EMD	SX0420-3
Sodium Dodecyl Sulphate (SDS)	≥99%	151-21-3	Millipore	428015
Sodium Hydroxide - NaOH	≥97.0%	1310-73-2	Thermo Fisher	S318- 1
Streptomycin	≥99.5%	69-57-8	ThermoFisher	15140122
Succinic Acid	≥99.0%	110-15-6	Millipore-Sigma	S9512
SYBR Green Dye	≥99.0%	163795753	Bio Rad	1725270
Tryptone N1	-	91079-40-2	OrganoTechnie	19553
Tween™20	≥40.0%	9005-64-5	Sigma-Aldrich	P1379
Zeocin	≥99.0%	11006-33-0	ThermoFisher	R25001

Commented [Ga13]: zum material gehören auch Zellen, Medien, Plasmide, usw.

Commented [i14R13]: still missing J-chain name and supplier

Commented [Ga15]: Materials comes before Methods

4.2. Equipment

Table 2: Equipment used in experiments; device, manufacturer, and model name

Device	Manufacturer	Model
AEX Column	Cytivia	5ml HiTrap Capto Q
Bench-top Centrifuge	Eppendorf SE	5425
Centrifugal Filter Unit	Millipore	Amicon Ultra-15
Chemiluminescent Imager	Azure Biosystems	Azure c600
Dialysis Cassette	ThermoFisher	3ml Slide-A-Lyzer
ECL Reagents	ThermoFisher	SuperSignal™ West Dura Pico
End-Over-End Rotor	ThomasSci	Roto-Mini™ Rotator Series
Fixed Angle Centrifuge	Thermo Electron Corporation	Sorvall RC6 Plus with Rotor 1500
FPLC Software	Cytivia	Unicorn 4.11
FPLC System	Cytivia	ÄKTA go
Fume Hood	LabConco	Protector XStream Laboratory Hoods
Gradient Mixer	Sigma-Aldrich	50ml Gradient Mixer
Hemacytometer	Thomas Scientific	Hemacytometer Bright Line
Imager	Azure biosystems	c300
Incubator	Nu-Aire	In-VitroCell ES NU-5700 CO2 Incubator
Maxiprep Kit	Invitrogen	PureLink HiPure Plasmid Maxiprep Kit
Microscope	Olympus	CX33
Miniprep Kit	Qiagen	QIAprep Spin Miniprep Kit
Nickel Resin	ThermoFisher	HisPur™ Ni-NTA Resin
Nickel-bead Column	Bio-Rad	Poly-Prep® Chromatography Columns
Nitrocellulose Membrane	Bio-Rad	0.45 µm
PCR Thermocycler	ThermoFisher	MiniAmp Thermal Cycler
Shake Flasks	Corning	125ml, 250ml, 1L
Shaking/thermal Incubator	Bellco Glass Inc.	221630
Silver Stain Kit	Thermo Fisher	Pierce™ Silver Stain Kit
Spectrophotometer	Thermo Scientific	NanoDrop one ®
Stericup	Millipore	500ml Stericup ®
Sterile Filter	Millipore	PES 0,2µm and PES 0,45um
Swinging bucket centrifuge	Beckman Coulter, Inc.	Allegra X-5
Syringe with 30G Needle	Becton, Dickinson, Co.	Precision Glide
Thermal Incubator	Fisher scientific	Dry bath incubator
Water treatment system	Barnstead	Nanopure Life Science UV/UF W TOC
WB Image Processing	National Institutes of Health	ImageJ, 1.53k; Java 1.8.0_172

4.3. Buffers & Media

Table 3: List of buffers used with name, chemical composition, and respective molarities

Name	Chemical Recipe
2XSDS loading buffer	100mM Tris pH6.8; 4 % SDS; 0.03% Bromophenol Blue; 20 vol% glycerol
2XSDS lysate buffer	100mM Tris pH6.8; 4 % SDS; 20 vol% glycerol
5% BSA	50µM Tris, 150µM NaCl, 0.1M HCl; 0.05% Tween™20; 5% BSA
Developer Solution	0.5mL of Silver Stain Enhancer with 25mL Silver Stain Developer
Elution buffer	provided by Thermo fisher, cat. No 21004
HEK293 expression medium	Freestyle™ 293 Expression Medium; Pen/Strep
HEK293 maintenance medium	Expi293™ Expression Medium; Pen/Strep, 200mM Glutamine
HEK293 transfection trial medium	Freestyle™ F17 Expression medium; + respective additive
LB medium	10g Tryptone, 10g NaCl, 5 grams yeast extract
Lysis Buffer	50% elution buffer; 50mM Tris pH6.8; 2 % SDS; 125mM DTT
MDCK MEM medium	MEM; Pen/Strep, 5%FBS, 200mM Glutamine
Nickel Elution Buffer	150mM imidazole in 1x D-PBS
Nickel Equilibration Buffer	10mM imidazole in 1x D-PBS
Nickel High Imidazole Buffer	500mM imidazole in 1x D-PBS
Nickel Wash Buffer	13mM imidazole in 1x D-PBS
PBS	1.4M NaCl; 27mM KCl; 80mM Na_2HPO_4; 18mM KH_2PO_4; to pH7.4 with 5M NaOH
PBST	1.4M NaCl; 27mM KCl; 80mM Na_2HPO_4; 18mM KH_2PO_4; to pH7.4 with 5M NaOH; 0.02% Tween™20
Ponceau S	5 vol% glacial acetic acid, 0.01 % Ponceau
Sensitizer Working Solution	50µL Silver Stain Sensitizer with 25mL MilliQ water
SilvStain Fixing	30% ethanol (C2H6O), 10% acetic acid (CH3COOH)
SilvStain Stop	5% acetic acid (CH3COOH)
SilvStain Wash	10% ethanol (C2H6O)
Stain Working Solution	0.5mL of Silver SNAP Enhancer with 25mL SilverSNAP Stain
TBST	50µM Tris, 150µM NaCl, 0.1M HCl; 0.05% Tween™20
TGM	50mM Tris; 1.5M glycine;
TGS	50mM Tris; 1.5M glycine; 1% SDS

Table 4: Media used for HEK293F expression and transfection in trial 1

Batch Trial (5ml)			
ID	**Name**	**Basal Media**	**Additives**
#1	F17 (no additives)	40ml F17	-
#2	Freestyle (GlutaMAX)	40ml Freestyle (GlutaMAX)	-

#3	8mM Glutamine	40ml F17	1,6ml 200mM Glutamine
#4	8mM Succinic Acid	40ml F17	37,8mg Succinic Acid
#5	8mM Asparagine	40ml F17 media	42,3mg Asparagine

Table 5: Media used for HEK293F expression and transfection in trial 2

Scale-Up Batch Trial (25ml)			
ID	**Name**	**Basal Media**	**Additives**
#1	F17 (no additives)	50ml F17	-
#2	Freestyle (GlutaMAX)	30ml Freestyle (GlutaMAX)	-
#3	8mM Asparagine	30ml F17	47,2mg Asparagine
#4	1% Tryptone N1	30ml F17	300mg Tryptone N1
Fed-Batch Trial (25ml)			
ID	**Name**	**Basal Media**	**Additives**
#5	10mM Glutamine/ 8mM Glucose	125ml F17 media	225,25mg D-Glucose
			5mL L-Glutamine 200mM
#6	125mM Glucose	8ml F17 media	180,2mg D-Glucose
#7	125mM Mannose	8ml F17 media	180,2mg D-Mannose
#8	125mm Galactose	8ml F17 media	180,2mg D-Galactose

Table 6: Media used for E.Coli transformation and plasmid production

Antibiotic	Used for	Working concentration	Stock concentration	Volume for Mini (5ml) & Maxi-Prep (250ml)
Ampicillin	J-chain	150µg/ml	100mg/ml	Mini: 7,5µl ; Maxi: 375µl
Zeocin	H-chain	30µg/ml	100mg/ml	Mini: 1,5µl ; Maxi: 75µl
Blastocidin	L-chain	75µg/ml	10mg/ml	Mini: 37,5µl ; Maxi: 1875µl

4.4. Cells, Plasmids & Antibodies

Table 7: List of cells, plasmids and antibodies used with name, notes, and supplier

Name	Notes	Supplier
E-Coli	DH5alpha (DH5a)	Thermo Fisher
HEK293F	Human Embryo Kidney Cells	American Type Tissue Culture Collection (Rockville, Maryland, USA)
MDCK plain	Mandin Darby Canine Kidney Cells	
MDCK11	Stably Transformed to express pIgR by Germino Lab at MCDB, UCSB	
pFUSE2ss-CLIg-hk	Light chain plasmid (IgA constant region)	Invitrogen
pFUSEss-CHIg-hA1	Heavy chain plasmid (IgA constant region)	Invitrogen
pIRESpuro3-human-J-chain-myc-His	Joining chain plasmid (IgA) containing pcDNA3.1/myc-His human J-chain insert	Stefan Lohse, Universitätsklinikum des Saarlandes, Germany
Rabbit anti-human IgA	-	Sigma-Aldrich
1F12 dIgA	Anti-cMet antibody	Meg Schimmel, UCSB
51D9 VL	Light chain insert (IgG variable region)	Integrated DNA Technologies (Coralville, Iowa, USA)
51D9 VH	Light chain insert (IgG variable region)	

5. Methods

5.1. Recombinant transformation of E.Coli

5.1.1. Transformation by heat-shock

Competent *E.Coli* cells were stably transformed by heat shock which creates pores in the cell wall through which the plasmid vector can enter and integrate to be amplified. For each of the anti-IL13 heavy, light, and joining chains, 20ng of recombinant plasmids was added to competent 50µl DH5α *E.Coli* cells thawn from -80°C. Cells were incubated for 20 minutes on ice and placed in a water bath at 42°C for 30 seconds. Cells were placed on ice for 5 minutes and 1ml of Luria-Bertani (LB) media was added before shaking for 60 minutes at 250rpm and 37°C. Cells were spun down at 4000rpm for 2 minutes and the pellet was resuspended in 100µl supernatant. These 100µl were spread out aseptically on prewarmed agar plates containing the respective antibiotic and incubated overnight at 37°C. The antibiotics used were 75µg/ml blasticidin for light chain, 30µg/ml zeocin for heavy chain and 150µg/ml ampicillin for joining chain plasmids. Sixteen hours later, a single colony was picked from each plate, added to 5ml LB media with antibiotic and shaken at 37°C overnight. Due to lengthy transformation processes, subsequent plasmid preps were started by streaking frozen glycerol stocks of transformed E.Coli cells and placing it in 5ml LB media with antibiotic.

Commented [Ga16]: give the concentration of the antibiotics

5.1.2. Mini-prep for plasmid purification

For plasmid DNA purification, harvested bacterial cells are lysed in NaOH-SDS, where SDS solubilizes phospholipids of the cell membrane. The addition of acidic potassium acetate neutralizes the lysate as high salt concentrations cause potassium dodecyl sulphate to precipitate while trapping DNA in salt-detergent complexes. Plasmid DNA then renatures, as it is small and covalently closed, and remains in solution [48]. Plasmid DNA of overnight culture was purified through a mini prep procedure following QIAprep Spin Miniprep Kit [81] (Qiagen, Hilden, GER). The purified plasmid was eluted from the column using 50µl TE buffer and its DNA concentration measured via NanoDrop.

Commented [Ga17]: give the reference of quiagen

Commented [Ga18]: give the concentration

5.1.3. Restriction digest of purified plasmid

The resulting plasmids are purified and digested by specific restriction enzymes which cut the plasmid at restriction sites flanking the recombinant insert for each dIgA chain. This releases the insert so that it can be identified on an agarose gel. Running cut samples through a gel allowed separation and identification of the recombinant insert. Fast digest buffer was added to the plasmid along with respective restriction enzymes and the 20µl reactions were incubated in a thermocycler at 37°C for 30 minutes.

Commented [Ga19]: this does not belong to transforation, it is a separate method (resctriction digest and agarose gel electrophoresis)

Commented [Ga20]: this is the method of resctriction digest

5.1.4 Gel verification of recombinant insert

A 1% agarose gel was prepared by adding 1g of agarose to 100ml of TAE buffer. This mixture was heated to dissolve agarose and when cooled, 10µl of SYBR green staining dye was added. The mixture was poured into a gel mould and once the gel had solidified, TAE buffer was added to submerge the gel. The 20µl digested plasmid DNA samples were loaded into the gel along with 3µl DNA Ladder. A current of 180V was passed across the gel for 50 minutes. The gel was imaged using a chemiluminescent imager. Successful transformation was confirmed by comparing band heights with known plasmid and insert sizes.

5.1.5. Maxi-prep for plasmid purification

1mL of the original 5mL bacterial culture was transferred to a shake flask with 250mL LB media with appropriate antibiotic, for plasmid production. Table 6 shows antibiotic concentrations added to culture media. These flasks were incubated at 37°C for 16 hours. In a scaled up version of the mini-prep procedure, plasmid DNA of 250mL overnight culture was purified following PureLink HiPure Plasmid Maxiprep Kit [82] (ThermoFisher, Waltham, USA). The purified plasmid pellet was dissolved in 500ml TE buffer, and its DNA concentration was measured via NanoDrop the following day.

Commented [Ga21]: this does not belong to gel electrophoresis

5.2. General cell culture

5.3.1. Cell thawing and freezing procedure

Cell-freezing is based on the principle that cells can retain their functions and for extended time periods at very low temperatures. It also prevents undesirable outcomes from continuous culture such as genetic drift, cell senescence and bacterial contamination. Cells are frozen in a cryoprotective agent such as dimethyl sulfoxide (DMSO) which reduces the mediums freezing point and allows a slower cooling rate. This reduces ice crystal formation which can be damaging to cells. To freeze adherent cells, they were washed with 5ml D-PBS and 2ml of 0,25% Trypsin in EDTA were added at 37°C. When cells released from the plate, they were resuspended in 8ml MEM medium and spun down at 1500 rpm for 2 minutes. The pellet was resuspended in MEM medium and cell count was taken to ensure viability was above 95%. A volume corresponding to $1x10^6$ cells per cryovial was spun down at 1500 rpm for 5 minutes. The pellet was resuspended in freezing medium made up of 40% fresh and 40% used medium as well as 10% DMSO. The cell suspension was transferred to labelled cryovials, stored long term at -80°C overnight and in liquid N_2. To freeze suspension cells, the same procedure was used except they did not have to be released. To thaw cells, cryovials were removed from liquid N_2, placed in a water bath at 37°C and shaken until 80% of cells had thawed. Cells were then transferred to a flask containing prewarmed medium and incubated. The following day, a medium change was done to remove DMSO.

5.3.2. Cell cultivation and maintenance

Cell maintenance was done to limit overgrowth and cell death. For MDCK cells, a medium change was done every three days. Every 9 days, they were split using the same method described above. The resulting cell pellet was resuspended in 10ml MDCK MEM medium of which 1ml was added to a new plate with 9ml MDCK MEM medium and incubated at 37°C and 5% CO_2. HEK293F cells were split when they reached $2x10^6$/ml. A volume corresponding to $3x10^5$/ml of the new flask volume was spun down at 1500rpm for 2 minutes. The pellet was resuspended in HEK maintenance media and incubated at 6% CO_2, 120rpm and 37°C.

5.3.3. Cell viability measurements

With the quality of cell samples being a key attribute for many processes in this thesis, viability measurements were performed on a routine basis. In the trypan blue exclusion assay, a 960 Dalton trypan blue molecule only enters the cells with compromised

membranes, i.e. dead cells. In this way, intracellular proteins of dead cells are stained blue and can be differentiated when performing a cell count under the microscope. Cell viability measurements were conducted by transferring 100µl cell culture to a 1,5mL tube combined with 100µl Trypan blue dye. 15µl of this mixture was injected to a Hemacytometer mounted with a coverslip. Under a microscope, the number of viable and dead cells was counted in 4 squares of the Hemacytometer. The average value was multiplied by 20.000 to find the total number of viable and dead cells per ml of culture.

5.3.3. Cell sampling and intensity measurements

Cell culture samples were taken at the point of harvest as well as during expression for media supplementation trials. For this, 100µl cell culture samples were taken and spun down in a bench-top centrifuge at 5200rpm for 5 minutes. The supernatant was combined 1:1 with 2x Sample Buffer and loaded onto an SDS gel along with a linear dilution of IgA standard with known concentration. The resulting western blot image was analysed using ImageJ software which assigns intensity values for each western blot band. The linear dilution was used to plot a standard curve and assign concentration values to samples.

5.3. Transient transfection

5.4.1. Standard transfection

Transient transfection is the process of introducing DNA to eukaryotic cells temporarily, without integration into the host genome. In this experiment, it was done to express dimeric IgA in HEK293-F suspension cells, a variant of human embryonic kidney cells, adapted to grow in serum free expression medium. Transfection was conducted using polyethylenimine (PEI) which allows the formation of nucleic acid-polymer complexes that adhere to the cell and are taken up by endocytosis. PEI is able to retain high cell viability when integrating large constructs [49] [7]. Incubation for all transfection trials was done at 37°C and 6% CO_2, while centrifugation was done using a swinging bucket centrifuge.

HEK293 cells were kept in culture and scaled up to 300,000 cells/ml in 1L liter flasks 2 days before transfection. This ensured that there were sufficient cells for transfection and that viability was above 97%. Shortly before transfection, a cell count was taken and a volume

containing 500 million cells was spun down for 2 minutes at 1500rpm. The cell pellet was resuspended in 15mL Freestyle™ 293 (GlutaMAX) medium. Table 8 shows the required reagents for transient transfection in 1L. Taken from this, 500 mL of transfection culture required 500 million viable cells, 625µg plasmid and 1,875mL PEI in a transfection volume of 25ml before being transferred to a 1L Erlenmeyer shake flask in the full culture volume.

Table 8: Reagents used for various transfection volumes

Culture volume final	Culture flask	Cells needed	Transfection volume	Plasmid mass	PEI (1 mg/mL stock)
15 mL	3 wells (each 5ml) of 6 well	15,000,000	0.75 mL	18.75 µg	56.25 µL
25 mL	125 mL	25,000,000	1.25 mL	31,25 ug	93,75 µL
100 mL	250 mL	$100x10^6$	5 mL	125 µg	375 µL
350 mL	1 L	$350x10^6$	17.5 mL	437.5 µg	1.3125 mL
500 mL	1 L	$500x10^6$	25	625	1.875 mL

The calculated DNA volumes were combined into a 15ml tube and filled with transfection media to make up a volume of 10ml. This was split between the two 15ml HEK cell suspensions and left to incubate at room temperature for 5 minutes. Meanwhile, 3,75mL PEI was added to 6,25mL transfection media and split between the two 20mL suspensions. The final 25ml were transferred to a 100mL bevelled shake flasks and left to incubate at 160rpm for 4 to 6 hours. The transfected culture was then transferred dropwise to a 1L shake flask containing 470ml prewarmed HEK293F Freestyle (GlutaMAX) medium with 5ml pen/strep. This 500ml suspension was left to incubate for 7 to 9 days at 140rpm. The suspension was then transferred to centrifuge tubes and spun down using a fixed-angle centrifuge at 9000rpm for 45 minutes. The resulting supernatant was sterile filtered using a Stericup™ attached to a 1L Shott Bottle and stored at 4°C.

Peptones are chemically undefined water-soluble protein hydrolysates containing peptides, amino acids, inorganic salts as well as lipids, vitamins, and sugars. While they have been shown to stimulate transfection efficiency and provide anti-apoptotic functions when added to growing cells, the mechanism for this is poorly understood [50] [51]. Regarding media feeding regimes, fed batch is the process of adding nutrients to the media during fermentation. This is typically done to replenish media with the precise nutrients that have become depleted and are inhibiting cell growth or protein expression as limiting substrates.

5.4. Concentration of cell supernatant

Supernatant concentration was achieved using a tangential flow filtration cassette which filtered the supernatant tangentially to the fluid flow thereby preventing the build-up of retentate. Inside the cassette are thin channels in a flip-flow recirculation path that provide high crossflow velocities at low pump speeds. The 100kDa molecular weight cut-off ensured that everything smaller is filtered out, retaining larger molecules such as IgA (MW>160kDa). Figure 5 shows that as the permeate containing spent media and small-size impurities is filtered out, the retentate becomes concentrated, reducing the number of reagents needed for subsequent purification steps [67].

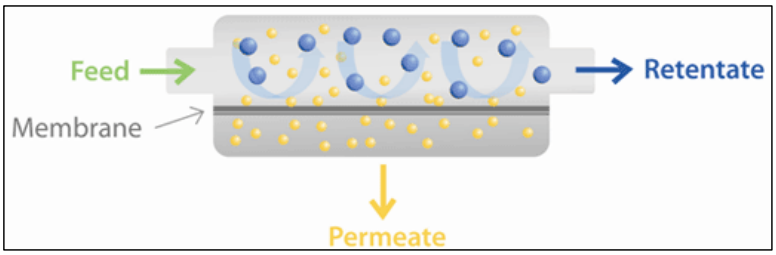

Figure 5: Schematic of tangential flow filtration

One liter cell supernatant was transferred stepwise into a 500ml sample reservoir, connected to a Vivaflow® 50R crossflow cassette through PVDF tubing. The inlet tube was placed through a pump of which the speed could be regulated manually. With the speed set at 2, the system pressure was monitored to stay below 2,5 bar. After retentate volume reduced to 30ml, 5ml of DI water were loaded directly into the cassette to capture residual antibody. The concentrated supernatant was transferred to a 50ml tube, sterile filtered through a 0,45µm filter and combined with 1:500 in volume of protease inhibitor and PMSF as well as 1:100 in volume of pen/strep. The VivaFlow system was rinsed with 500ml Milli-Q water and 200ml NaOH and the cassette was stored in 70% ethanol.

5.5. Nickel-bead affinity chromatography

For further purification of IgA from the concentrated supernatant, his-tagging was used whereby a polyhistidine tag is included in the proteins genetic sequence so that histidine residues (His-tag) are expressed. When agarose beads loaded with nickel ions are added to supernatant, the Ni^{2+} ions coordinate with the histidine side chains. The supernatant is equalized with a low concentration of imidazole which competes with low affinity binding proteins to reduce bead contamination. When the cell-bead mixture is loaded onto a gravity column, the protein-bound beads are caught by a porous polyethylene bed while the remaining, supernatant flows through. Using a gradient of low to high imidazole, the disulphide bonds between His-tag and Nickel-ions are gradually broken, causing the protein to be released. This can occur as imidazole binds to a functional group on histidine residues thereby competing with Ni^{2+} ions.

The concentrated supernatant was mixed with an equal amount of equilibration buffer (EqB). A volume equal to 1,5% of the concentrated supernatant volume was taken in resin slurry and added to two 1,5ml tubes. The tubes were centrifuged for 2 minutes at 2500rpm using a bench-top centrifuge, and the supernatant discarded carefully. The resin bed was resuspended in 500µl EqB and centrifuged in the same way. This step was repeated, and the resulting resin bed was resuspended in 500µl antibody: EqB mixture. The suspension was added back into the respective 50ml tubes which were placed on an end-over-end rotor and spun for 16 hours at 15 rpm. Then, a Poly-Prep® column was fixed to a stand with a 100ml beaker under it. The antibody:EqB mixture was transferred stepwise to the column and the flowthrough collected. Then, 2,5ml Elution buffer (EB) was added to the right and 2,5ml wash buffer (WB) to the left column of a gradient mixer. A stir bar was added to each mixer-column and the mixer placed on a stir plate with a tube connecting the right mixer-column to the chromatography column through a rotor. The rotor was turned on and the valves open from left to right creating a gradient as WB flowed out before mixing with EB. As the gradient dripped out and into the chromatography column, rotor speed was adjusted to ensure that the resin bed was covered by gradient. As the eluate dripped out of column, it was captured in 0,5ml elutions. A final elution was done using 0,5ml high imidazole buffer.

5.6. SDS PAGE

In sodium dodecyl sulphate–polyacrylamide gel electrophoresis (SDS PAGE), the addition of SDS to samples acts as a surfactant, giving proteins a negative charge. The application of an electric current causes protein to migrate from the cathode to anode with different speeds based on their molecular weight. In this way, samples are separated into their constituent proteins. The percentage of acrylamide added to the gel depends on the size of proteins to be separated as it thickens the gel and therefore slows protein migration. Since samples in this study were tested for dIgA, with a size of 200kDa in monomeric and 400kDa in dimeric form, 6% gels were used since they are recommended for proteins larger than 130kDa. For the procedure, the gel was fixed into an SDS cassette and placed into a chamber filled with TGS buffer. Samples were mixed with 2x SB and up to 30µl was loaded into each well. 3µl prestained 250kDA protein ladder with human low-density lipoprotein (LDL) was added to the first well. The chamber was run with a 100 volt current for 120 minutes.

Commented [Ga22]: giving a negative charge

5.7. Western Blotting

Western blotting is an analytical technique to visualize and quantify specific proteins in a sample. Following separation via SDS PAGE, proteins are electrophoretically transferred to a hydrophobic membrane. The membrane is then probed by a fluorescent antibody which recognizes membrane-bound target proteins and allows visualization.

The SDS PAGE gel was transferred to a nitrocellulose membrane and placed between two pieces of filter paper, two sponges and a clamp before being placed into a transfer chamber with TG buffer. The chamber was placed into an ice box on a stir plate with a stir bar to limit methanol in TG buffer heating up. The gel bands were transferred by a 100 volt current for 105 minutes. The membrane was stained with Ponceau solution and the LDL band at 500kDa was marked with a pencil. The membrane was incubated in TBST at 4°C and the following day washed three times for 5 minutes with TBST. A rabbit anti-human IgA antibody was diluted 1:10.000 in 1% BSA blocking buffer and 5ml were added to the membrane for 1 hour. The membrane was washed three times with TBST for 5 minutes. A pair of 1ml HRP substrate aliquots were combined in a 1,5ml tube and transferred onto the

membrane. On the chemiluminescent imager, the gel was imaged with increasing exposure times until the bands were clearly visible. The ladder was imaged using the built in LED.

5.8. Silver Staining

Silver staining is the process of staining all proteins in a sample, as silver ions bind negatively charged side chains on proteins becoming selectively reduced and visible. This technique is commonly used to visualize glycosylations as they form separate bands on stained gels. In addition, it can be used to assess sample purity as it visualizes contaminant proteins.

SDS gels were washed in two cycles of DI water for 5 minutes each before incubating it in two cycles of 20ml fixing solution for 20 minutes each. This denatures the proteins, removes SDS and limits protein diffusion. Two cycles of 20ml washing solution were then added for 5 minutes each before adding 25ml Sensitizer working solution for 1 minute. The gel was washed with two changes of DI water for 1 minute each and incubated with 25ml Stain working solution for 5 minutes. The gel was washed with two changes of MilliQ for 20 seconds each and 25ml developer Solution was added. The gel was tilted until all bands had been stained and two cycles of 20ml stop solution were added and incubated for 15 minutes before storing in Milli-Q water. The gels were imaged using c600 chemiluminescent imager.

5.9. Dialysis

Buffer exchange is an essential method before and after anion exchange chromatography (AEX). Before AEX because it removes imidazole, which would otherwise increase the absorbance values during elution. More importantly, the buffer controls the proteins net charge whereby a buffer with a pH higher than the proteins pI makes it negatively charged and vice versa. This is essential for AEX since it separates negatively charged proteins. After AEX, dialysis ensures that the antibody is buffered and stable for longer amounts of time.

For dialysis, 3ml Slide-A-Lyzer cassettes were immersed in pH 7.4 PBS for 1 minute. After removing the cassette and drying the membrane, pooled dIgA elutions were filled into a syringe. The needle was inserted into one port and the sample was injected slowly into the membrane. Air was removed using the syringe, ensuring not to touch the membrane. The

cassette was then placed into 1 liter pH 7.4 PBS (dialysis solution) in a beaker on a stir plate with a stir bar. After 2 hours, the dialysis solution was replaced and after another 2, the cassette was left to dialyze overnight. The sample was then removed by injecting air into the membrane, tilting the cassette to draw out the sample and transferring it to a 5ml tube.

5.10. Anion-Exchange chromatography

Proteins contain positive & negatively charged chemical groups which makes ion exchange chromatography (IEX) favourable for their purification as it separates based on charge. In this study, anion exchange chromatography (AEX) was used where negatively charged dIgA binds a positively charged anionic column. The adsorptive properties of charged proteins make them bind to a stationary phase of opposite charge. By gradually increasing the salt concentration, proteins with a weak negative charge, and therefore lower binding affinities will elute first and the protein of interest is gradually released off the column. In this way, process-related impurities such as host cell proteins and endotoxins with weaker or stronger binding affinities, can be separated. By running the AEX using a fast protein liquid chromatography (FPLC) system, UV absorbance and conductivity measurements could be recorded and analysed during protein elution.

For AEX, a 5ml HiTrap AEX column was fixed in an ÄKTA FPLC system. UV absorbance, pH and conductivity of the effluent stream were monitored using Unicorn 6.3 software. The column was then washed with 5ml 1x PBS (pH 7.4), 5ml 1M NaCl in PBS (pH 7.4) and again 5ml 1x PBS (pH 7.4) until the UV baseline, eluent pH and conductivity stabilize. Dialyzed elutions were loaded onto the column at a flowrate of 0,5ml/min. The column was washed with 10ml 1M NaCl in PBS (pH 7.4) and the flowthrough was collected. dIgA was eluted using a linear gradient volume of 25ml and increasing salt concentrations up to 0,45M NaCl, and captured in thirty-five 0,5ml fractions. The column was washed with 5ml 1M NaCl and re-equilibrated with 10ml 1x PBS until UV, pH and conductivity stabilized. The column was washed with 2ml MilliQ water followed by 2ml 20% ethanol before sealing it.

5.11. PNGase degylcosylation

PNGase enzyme (peptide:N-glycosidase) cleaves N-linked oligosaccharides of glycoproteins, leaving them intact for further analysis. For denaturation conditions, 1 to 20µg glycoprotein

was combined with 1µl Glycoprotein Denaturing Buffer and H_2O in 10µl reaction volume. The sample was heated at 100°C for 10 minutes and chilled on ice before centrifuging for 10 seconds. 2µl GlycoBuffer 2, 2µl 10% NP-40 and 6µl H_2O were added. 1µl of PNGase F was then added to the sample before gently mixing and incubating it at 37°C for 1 hour. For the non-denaturing reaction, 1 to 20µg glycoprotein was combined with 2µl GlycoBuffer 2 and H_2O in 20µl reaction volume. 2µl PNGase F was added, and the reaction incubated at 37°C for 4 to 24 hours. In theory, the incubation time altered the level of glycosylation.

5.12. Transcytocis assay

Transcytocis refers to a cellular transport mechanism in which large molecules are transported across the inside of a cell. In the human body, transcytocis represents an essential function to transport dIgA across epithelial surfaces of organs so that it may bind pathogens, seen in

Figure 3. During transcytocis, a section of pIgR is cleaved and attached to dIgA to protect it from proteolytic cleavage. The ability of dIgA to be transcytosed can be determined in-vitro through an assay which mimics the pIgR expressing epithelial layer. Figure 6 is a schematic representation where dIgA is added to the basolateral well, pIgR is expressed on the cell

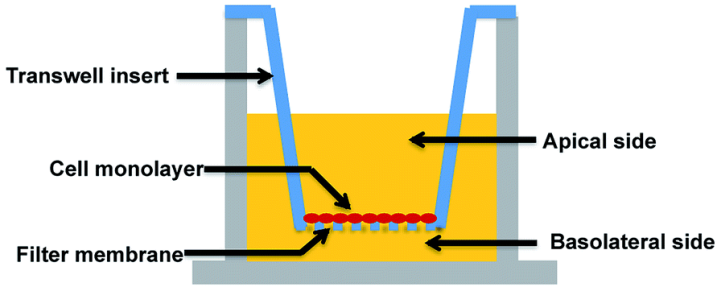

monolayer and samples are taken from the apical well [68].

Figure 6: Schematic of transwell-based approach for in-vitro transcytocis

The first step for the assay was to thaw adherent Mandin Darby Canine Kidney, MDCK11 and MDCK plain cells using MDCK MEM medium in 10cm plates. Once the cells had almost reached confluence, they were released from the plate by aspirating the medium, washing them with 8ml D-PBS (1x), adding 2ml 0,25% trypsin/ EDTA and incubating them at 37°C

until cells released from the plate. Then, 8ml fresh MEM was added to resuspend cell clumps. The cell suspension was transferred to a 10ml tube and centrifuged for 2 minutes at 1,500rpm. The supernatant was discarded, and the cell pellet resuspended in 10ml MEM. A sample of this suspension was used for a cell count and the suspension was diluted to 50.000 cells/ml. Of this, 500µl was added to the apical well of each transwell. 500µl of MEM medium was added to the basolateral well and the transwell plate was incubated at 37°C. After 3 days, a leak test was run by adding 300µl complete medium to the apical and removing 300µl from the basolateral well. The next day, transwells were inspected to see if the volume had equalized. If it had not, the leak test was successful, meaning that MDCK cells had formed a seal, and the transcytocis assay could begin. Purified 51D9 dIgA, control human IgA and supernatant IgA were diluted in MEM in a concentration of 10µg/ml. Spent media was removed from the transwells and 500µl of each sample dilution was added to the basolateral well of one MDCK plain and one MDCK11 transwell. 500µl MEM medium was added to the apical well and the transwell plate was incubated at 37°C. 100µl apical well samples were taken at selected time points and replaced by 100µl prewarmed MEM.

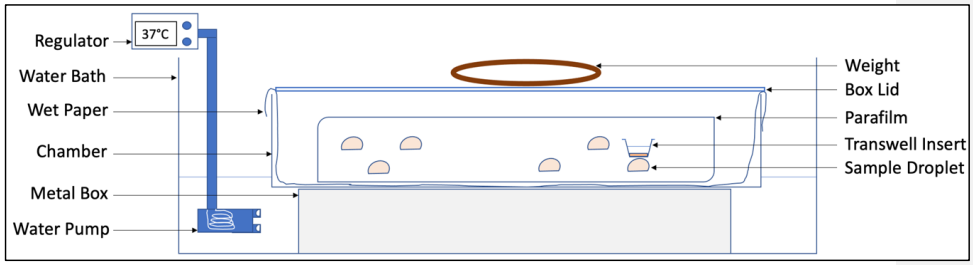

Figure 7: Schematic of Droplet Transcytocis Setup

An alternative was tested where the confluent transwell insert seen in Figure 6, was placed on a droplet containing higher concentrations of the IgA sample, facilitating pIgR-dIgA contact. For this droplet transcytocis assay (DTA), purified dIgA and IgA supernatant were diluted in 50µl MEM in a concentration of 80µg/ml. A piece of parafilm was placed on top of wetted tissue paper inside a rectangular box, creating a humid chamber which was placed in a water bath at 37°C. For the assay, two 25µl droplets of each diluted IgA sample were

placed directly onto parafilm, one for MDCK plain and one for MDCK 11 transwell inserts. Spent media was removed from inserts and 500µl fresh MEM medium was added to the apical well before transferring transwell inserts onto the droplets of diluted dIgA on parafilm in the humid chamber. 100µl apical well samples were taken at selected time points for analysis and replaced by 100µl prewarmed MEM medium. Figure 7 shows this setup.

5.13. Immunoprecipitation

To enrich dIgA of apical well samples, they were immunoprecipitated. In a similar way to the Nickel purification step, this was done by adding 40µl equilibrated nickel beads to the 100µl apical well samples. Samples were rotated for 16 hours at 15rpm in an end-over-end rotator and centrifuged at 700g for 2 minutes before removing the supernatant using a syringe with a 30G needle. Bound IgA was eluted off the beads using 20µl 2xSDS Sample Buffer. Samples were spun at 700g for 2 minutes and dIgA containing supernatants were transferred to new tubes using the syringe. In this way IgA was concentrated by a factor of 5 and samples could be run on a western blot for visualization. A non-reducing and a reducing western blot were run. The non-reducing consisted of loading immunoprecipitated samples directly onto a 6% SDS gel since they had been eluted with sample buffer. For the reducing condition, 1µl dithiothreitol (DTT) was added to 10µl IP sample, vortexed and the mixture was incubated on a 100°C heat block for 5 minutes before loading the samples on a 10% gel.

6. Results

Commented [Ga23]: PCR Ergebnis? rekombinantes Plasmid?

Commented [i24R23]: explain plasmid setup etc.

Commented [Ga25]: explain the components of the plasmid

6.1. Transformation of recombinant plasmids

In the following work, anti-IL13 dIgA is referred to as 51D9, and anti-cMet dIgA is referred to as 1F12 . Recombinant plasmid generation of the 51D9 and 1F12 light and heavy chains was performed by the thesis supervisor Ms. Schimmel. This was done by ligating the antibodies' variable region insert with a backbone plasmid for the antibodies' constant region.

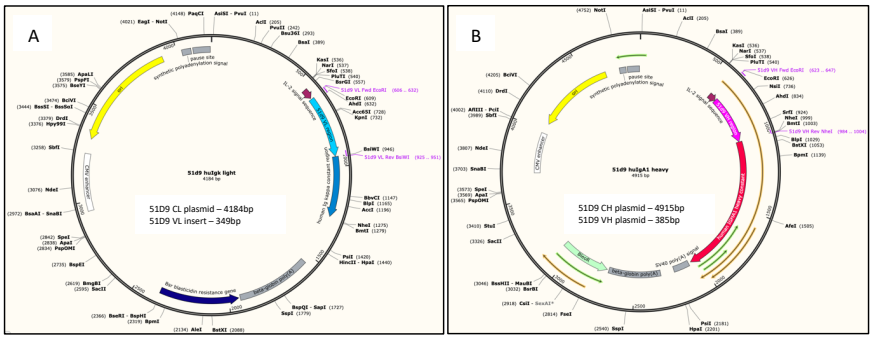

Figure 8: Sequence map of 51D9 light and heavy chain backbone plasmids

Figure 8 shows the recombinant plasmids generated for the 51D9 light chain (Figure 8A) and heavy chain (Figure 8B). It includes the adjacent variable and constant regions, an origin of replication (ori) to initiate replication and an enhancer region. It also shows restriction sites which were used to cut and ligate the plasmid with the variable region insert. The antibiotic resistance gene ensured that only cells which took up the plasmid could proliferate on antibiotic containing media. It also shows the plasmid and insert sizes being 4184bp and 349bp, respectively for the light and 4915bp and 385bp, respectively for the heavy chain.

6.2. Verification of recombinant plasmids

Commented [Ga26]: immer zuerst mit einem Satz beginnen und dann die Abbildung einfügen

The recombinant plasmids for *51D9* heavy, light, and joining chains provided by Ms. Schimmel were transformed into competent *E.Coli* cells for amplification. The amplified

plasmids were then purified, and their inserts verified using an agarose gel. Table 9 outlines the reagents used to cut the purified plasmids in 20µl reactions. For each plasmid, four reactions were run, namely an uncut, where no enzymes were added, two single cuts with either the 1st or the 2nd enzyme and a double cut with both restriction enzymes.

Table 9: Outlining the reagents used to digest purified plasmid DNA for gel verification

Plasmid DNA	1st Restriction enzyme	2nd Rest. enzyme	Fast Digest Buffer	H_2O (uncut)	H_2O (single)	H_2O (double)
2µl J-chain (1099)	1µl *Eco*RI	1µl *PvuI*	2µl	16µl	15µl	14µl
2µl H-chain (1032)	1µl *EcoRI*	1µl *NheI*	2µl	16µl	15µl	14µl
2µl L-chain (1033)	1µl *EcoRI*	1µl *Pfi23II*	2µl	16µl	15µl	14µl

The full and digested plasmids can be seen on the agarose gel picture in Figure 9. For each plasmid, single cuts show similar band heights as they both cut the plasmid once, thereby generating a linear structure for the whole plasmid seen at 4800bp for the heavy and 4100bp for the light chain. The double cut lanes show the plasmid insert where the heavy and light chain insert can be seen around 380bp and 350bp, respectively. These sizes correspond to those seen in

Figure 8, indicating successful transformation. For the joining chain. When looking at uncut lanes, it seems that most of DNA is supercoiled with thickest bands showing between 3 and 4 kBp. This topology is favoured for transfection as circular and linear DNA are vulnerable to degradation [52]. Double cut lanes for the heavy, light and joining chain also show additional bands apart from those identified. These could represent non-specific cutting by restriction enzymes, which happens less frequently and explains weaker bands. The joining chain plasmid has a known size of 5836bp and the insert a size of 828bp. While the plasmid size corresponds to the single lanes, the double cut lane shows two bands around 2000bp and 4000bp. This is because restriction enzymes did not cut out the joining chain insert but instead cut the plasmid in half.

Commented [Ga27]: restriction enzymes are written in italic (kursiv)

Commented [i29R28]: without eepetive things

Commented [i30R28]: Titel above

Commented [Ga31]: there are additional bands seen in the double digested plasmids, explain them as well

Commented [i32]: can go out

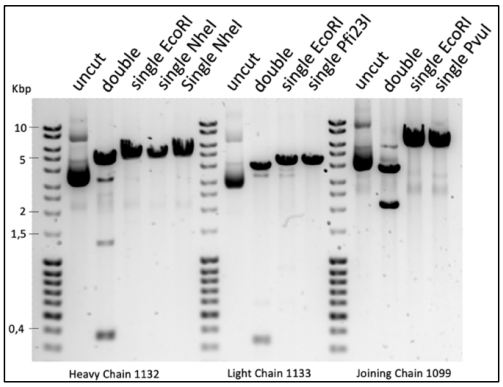

Figure 9: Image of agarose-gel separated 51D9 dIgA plasmids

6.3. Combining of recombinant plasmids for transfection

Table 10 gives an example of the plasmid samples used for transfection batch *195. The second row shows the plasmid ID, specific to the target IL13 for light and heavy chains. The third row shows the amount of DNA needed for two batches of 500ml, based on the general 1:2:2 ratio optimized for dimer assembly. The fourth row shows which sample was used and its purity. The latter was the key criteria for choosing which sample to use, as absorbance values should not surpass 1,95 for A280/A260 (A280) and should be higher than 2,30 for A230/A260 (A230). By co-transfecting with plasmids for the light, heavy and joining chains, cells had all the DNA necessary to assemble monomeric and dimeric IgA.

Commented [Ga33]: criteria

*Table 10: Example of plasmid preps used for transfection batch *195*

Expression conditions	Heavy chain	Light chain	Joining chain	Total DNA (2x 500mL)
Plasmid ID	#1132	#1133	#1099	
Amount of DNA based on 1:2:2 (for 2x 500mL)	250 µg	426 µg	584 µg	1,250 µg
DNA preps used/dates:	1132A (3/4/22) A280: 1,92 A230: 2,31	1133B (20/10/22) A280: 1,95 A230: 2,35	1099A (28/12/21) A280: 1,89 A230: 2,45	
DNA concentration	1193ng/µl	876ng/µl	1500ng/µl	
Calculated DNA volume	168µl	389µl	311µl	868ul

6.4. Growth rates during IgA expression

Commented [Ga34]: Einleitungssatz

Production remained flexible for optimization through the use of transient transfection methods avoiding the laborious process of creating stably expressing cells for every target. Since these HEK293F cells have been optimized to grow in serum-free medium, they could be transferred to larger volumes and left to express until growth reached a plateau. Growth curves for individual transfection batches were generated by taking daily cell viability measurements and plotting viable cell density and percentage dead cells against hours post transfection. As can be seen from Figure 10, the culture experiences substantial cell death in the first 24 hours post transfection (HPT) as viable cell density (VCD) decreases from 500.000 cells/ml to 100.000 cells/ml while the percentage of dead cells (DC%) increases from 3% to 80%. In the following 48 hours, VCD remains stable and begins to increase exponentially at 96 HPT, reaching its maximum of 2.065.000 cells/ml at 230 HPT. In the meantime, DC% decreases linearly, reaching its minimum of 20% at the point of harvest.

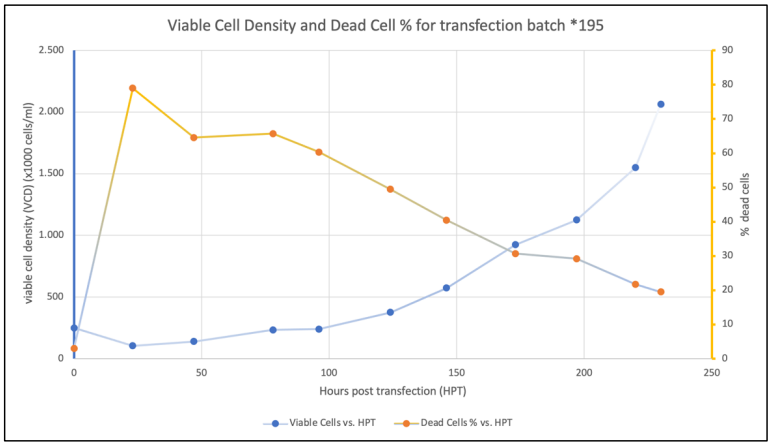

*Figure 10: Growth curves for transfection batch *195*

6.5. Key output parameters from transient transfection

6.5.1. Comparison of batches *189 to 195

To compare transfection batches, a set of output parameters were chosen based on cell viability measurements. Population doubling time indicated overall cell growth over time,

while maximum cell density and biotic potential gave insight into the cells' peak performance in terms of weight and proliferation, respectively. Table 16 (Appendix A) shows the equations used to calculate these parameters. Band intensities were measured as a quick assessment of IgA content in supernatant and purified elutions. By loading IgA standards, knowing the concentrations, a titration curve was drawn with the corresponding intensity values. The equation of the resulting trendline was used to calculate the concentration of supernatant samples from band intensity measurements. In the following analysis, significance is inferred when values are over one standard deviation (SD) higher or lower than average for transfection batches 189 to 195.

Table 11 shows transfection conditions as well as cell culture and expression parameters for seven standard transfection batches *189 to *195. Here it can be seen that the quality of plasmids did not vary greatly between batches, deviating only slightly from the average values. The cell density prior to transfection varied substantially, with an average at 2,39 million cells/ml ±0,5 and so did transfection incubation time averaging at 5,21 h ±0,7. In terms of cell culture parameters, batch *191 showed the highest maximum cell density with 4,05 million cells/ml and highest biotic potential with 4,33 cells/day/cell, as well as the lowest population doubling time with 1,26 days per population doubling. In contrast, batch *191 shows a low estimated dIgA concentration of 0,3µg/µl and low band intensities of purified elutions. When examining dIgA band intensities, batch *192 shows the highest values among all transfections with an estimated 4,86µg/µl dIgA in supernatant and IgA band intensity of 202.867 after nickel elution.

*Table 11: Transfection conditions and output parameters in transfections *189 to *195*

	Transfection Conditions					Cell Culture Parametres			Expression Parametres		
1000ml Transfection	Plasmid Quality 280/A260			Cell density pre-transfection (x1000 cells/ml)	Transfection Time (hours)	Maximum Cell Density (x1000 cells/ml)	Maximum growth rate (rmax)	Population doubling time (days)	Supernatant at harvest		Ni-purified Elutions
Batch Number	H Chain	L Chain	J Chain						dIgA band intensity	IgA conc. (in ug/ul)	IgA band intensity
Batch *189	1,92	1,95	1,93	1.825	5,5		-	-	56.477	3,93	192.665
Batch *190	1,92	1,96	1,96	3.190	5	885	1,08	3,61	31.095	2,43	-
Batch *191	1,93	1,96	1,95	2.245	6	4.045	4,33	1,26	6.845	0,30	31.621
Batch *192	1,93	1,96	1,93	2.260	6	2.470	1,89	1,65	44.469	4,86	202.867
Batch *193	1,96	1,93	1,91	2.350	4	1.890	2,60	1,58	38.533	4,14	170.107
Batch *194	1,92	1,91	1,92	2.950	5	1.020	2,92	1,42	1.279	0,22	146.115
Batch *195	1,92	1,91	1,92	2.440	5	2.065	1,11	3,14	-	-	-
Average	1,93	1,94	1,93	2.390±500	5,21±0,7	2.062±1149	2,32±1,24	2,11±1	29.783	2,65±2	148.675

Legend		
		Favourable
		Unfavourable

6.5.2. Media supplementation – Trial 1

Commented [i35]: only principle - title for result

Batch supplementation of culture media is used to provide cells with specialized compounds they require for cell growth and protein synthesis, at the start of fermentation. This method has proven effective to manipulate metabolic pathways and control glycan composition [Pazitna, 2020, Villacrés, 2021]. For the first media supplementation trial, transfection volumes were scaled down to 0,75ml and reagent volumes adjusted based on Table 8. In preparation, expression media listed in Table 4 were made by dissolving additives in a 50ml falcon tube with media and sterile filtering through a 0,2 µm filter. Transfection reactions in this trial, were done in 12 well plates and each well was split between 3 wells of a 6 well plate for expression. For clarity, see Appendix B for a depiction of conditions.

A small-scale batch trial was planned to test the effect of Glutamine, Asparagine and Succinic acid on cell viability and productivity during IgA expression. Freestyle 293 (GlutaMax) and Freestyle F17 (F17) expression media were the positive and negative controls respectively. In Trial 1, a number of compounds were tested in batch supplementation at 5ml expression volumes. The same cell culture and expression parameters were calculated using cell viability and band intensity measurements. Table 12 shows the condition of F17 +8mM Asparagine, yielding most promising results with significantly higher maximum cell density, biotic potential, and significantly lower doubling time. This trend is reflected in band intensities with the F17 +8mM Asparagine condition showing highest values in dIgA intensity and estimated IgA concentration. While succinic acid supplementation yields highest IgA concentrations, most is in monomeric form.

Table 12: Key cell growth parameters and western blot band intensities for IgA in Trial 1

	Cell Culture Parametres			Expression Parametres		
Batch Trial 1 5ml Transfection				Supernatant WB Band Intensity after 96 hours		
Conditions tested	Maximum Cell Density (x1000 cells/ml)	Biotic potential (rmax)	Population doubling time (days/pop doub)	dIgA	mIgA	IgA concentration (in ug/ul)
F17 + no additives	670	0,22	8,10	27.711	12.074	1,29
Freestyle (GlutaMAX)	833	0,35	4,76	37.016	5.417	1,18
F17 + 8mM Asparagine	1.045	0,84	3,31	44.237	4.857	1,60
F17 + 8mM Glutamine	778	0,48	4,64	24.977	8.585	0,46
F17 + 8mM Succinic Acid	642	0,73	7,56	32.004	11.735	1,82
Average ± Std. deviation	793±160,77	0,53±0,26	5,67±2,06	33.189	8.533	1,27±0,52

Legend		Favourable
		Unfavourable

6.5.2. Media supplementation – Trial 2

Commented [i36]: only principle - title for result

In the second trial, a scale-up of batch supplementation with Asparagine and Tryptone N1 was conducted with positive and negative controls such as in the first trial. Transfection volumes were scaled up to 1,25ml and reagent volumes adjusted based on Table 8. Expression media listed in Table 5 was made in preparation. Transfection reactions were done in 12 well plates and each was transferred to a 125ml culture flasks for expression. See Appendix D for clarity. In standard transfection batches 189 to 194 and Trial 1, substantial cell death was observed in the first 24 hours post transfection. To remedy this, batch supplementation with Tryptone N1 was used in this trial due its supplementation providing anti-apoptotic properties and improvement on cell productivity in previous studies [50] [51]. Table 13 shows that F17 +8mM Asparagine yields the highest maximum cell density, growth rate and lowest doubling time. In terms of band intensities, the condition of TF17 +1% Tryptone N1 shows the highest values in IgA intensity and estimated IgA concentration, both after 135 and 168 hours. In terms of growth rates in this trial, the TN1 condition shows two anomalies: viable cell density increases linearly compared to exponentially for other conditions; and percentage dead cells starts low and increases during expression, with the opposite trend seen for others (Appendix G).

Table 13: Expression parameters and IgA band intensities for 25ml batch transfection Trial 2

	Cell Culture Parametres			Expression Parametres					
Batch Trial 2 25ml Transfection	Maximum Cell Density (x1000 cells/ml)	Biotic potential (cells/day/cell)	Population doubling time (days/pop doub)	Supernatant WB Band Intensity after 135 hours			Supernatant WB Band Intensity after 168 hours		
Conditions Tested				dIgA	mIgA	IgA conc. (in ug/ul)	dIgA	mIgA	IgA conc. (in ug/ul)
F17 + no additives	6.780	2,25	1,55	34.951	8.448	0,38	29.569	11.512	0,36
Freestyle (GlutaMAX)	3.306	0,85	2,31	41.721	15.555	0,51	46.642	17.011	0,57
F17 + 8mM Asparagine	7.460	2,54	1,49	40.769	13.181	0,48	40.194	16.650	0,51
F17 + 1% Tryptone N1	2.133	0,38	4,46	48.415	18.688	0,60	46.709	19.499	0,60
Average ± Std. deviation	4.920±2600	1,50±1,05	2,45±1,39	41.464	13.968	0,50±0,09	40.779	16.168	0,51±0,10

Legend	Favourable
	Unfavourable

In a parallel fed-batch trial, fed-batch supplementation with Mannose and Galactose was tested in 25ml expression volumes four and six days post transfection. Expression was started using F17 media supplemented with 10mM Glutamine and 8mM Glucose and fed with 2ml of either 125mM Glucose, Mannose and Galactose to restore an overall 8mM

molarity of depleted sugars. Fed-batch supplementation with glucose was used as a positive and fed-batch F17 media as a negative control. Table 14 shows that feeding with galactose produced significantly higher and feeding with mannose significantly lower maximum cell densities. Feeding with mannose also yielded significantly lower biotic potential. Another notable finding was that for all conditions, IgA band intensities decreased between two timepoints, except for F17 G/G +8mM Glucose which experienced a slight increase.

Table 14: Expression parameters and IgA band intensities for 25ml fed-batch in Trial 2

	Cell Culture Parametres			Expression Parametres					
Fed-Batch Trial 2 25ml Transfection	Maximum Cell Density (x1000 cells/ml)	Biotic potential (cells/day/cell)	Population doubling time (days/pop doub)	Supernatant WB Band Intensity after 135 hours			Supernatant WB Band Intensity after 168 hours		
Conditions Tested				dIgA	mIgA	IgA conc. (in ug/ul)	dIgA	mIgA	IgA conc. (in ug/ul)
F17 G/G no add	6.920	3,45	1,29	34.940	18.448	0,34	29.467	11.456	0,29
F17 G/G + 8mM Glucose	7.426	2,93	1,36	36.966	18.153	0,35	38.277	17.787	0,36
F17 G/G + 8mM Galactose	8.520	2,98	1,35	38.207	18.005	0,36	31.731	14.624	0,29
F17 G/G + 8mM Mannose	5.880	1,96	1,55	40.579	18.763	0,38	32.019	14.335	0,29
Average ± Std. deviation	7.187±1098	2,83±0,63	1,39±0,11	37.673	18.342	0,36±0,02	32.874	14.551	0,30±0,03

Legend		
		Favourable
		Unfavourable

6.5.3. Media supplementation – Trial 3

Commented [i37]: only principle - title for result

In the third trial a scale-up of batch supplementation with Tryptone N1 was done, with Freestyle 293 (GlutaMAX) media as the positive control. In Trial 3, only the condition of batch supplementation with 1% Tryptone N1 (TN1) was carried forward and scaled up to 350ml expression volumes in order to compare it with standard conditions. Transfection volumes were scaled up to 17,5ml in 125ml shake flasks with reagent volumes adjusted based on Table 3 and expression was done in 350ml media 1L shake flasks. In preparation, 4g Tryptone N1 was added to 400ml F17 media and sterile filtered via 0,2µm filters. Table 15 shows that the control condition of using Freestyle (GlutaMAX) media achieved higher cell densities and growth rates as well as shorter doubling time than TN1. When looking at band intensities, TN1 supplementation yielded stronger IgA monomer and dimer bands than for the control condition.

Table 15: Expression parameters and IgA band intensities for 350ml batch in Trial 3

	Cell Culture Parametres			Expression Parametres		
Batch Trial 3 350ml Transfection	Maximum Cell Density (x1000 cells/ml)	Biotic potential (rmax)	Population doubling time (days/pop doub)	Supernatant WB Band Intensity after 9 days		
Conditions tested				dIgA	mIgA	IgA conc. (in ug/ul)
Freestyle (GlutaMAX)	6.572.000	1,44	2,49	3.716	1.405	0,82
F17 + 1% Tryptone N1	4.000.000	0,60	4,06	18.994	6.534	10,65
Average ± Std. deviation	793±160,77	1,02±0,59	3,28±1,11	33.189	8.533	5,74±6,95

Legend		
		Favourable
		Unfavourable

Growth rates of 1% Tryptone N1 supplementation were compared with positive control of Freestyle (GlutaMAX) by looking at viable cell density and % dead cells during expression.

Figure 11 reveals that for the control, growth and decay rates follow a similar trend than standard transfection batches such as *195 in Figure 10. Cell growth is in lag phase until 96 HPT before rising exponentially until the point of harvest. The percentage of dead cells rises rapidly post transfection and slows gradually until reaching a plateau of 15% at 120 HPT. For the condition of Tryptone N1, viable cell density rises incrementally before experiencing similar exponential growth at 120 HPT. The percentage of dead cells remains below 4% until 120 HPT where it rises exponentially until the point of harvest.

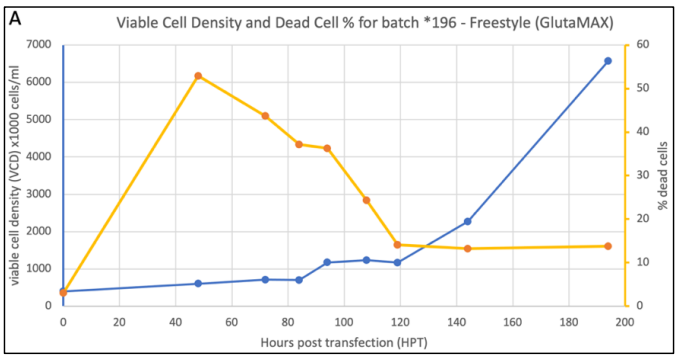

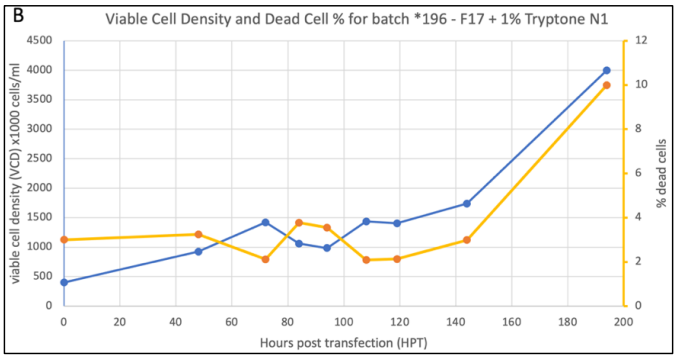

Figure 11: Growth curves for transfections in Trial 3

6.6. Nickel bead chromatography

After harvesting and concentrating the supernatant of transfection batches *189 to *195, it was incubated with nickel beads to purify dIgA. This was made possible by a histidine tag, expressed on dIgA's joining chain which nickel beads could bind. dIgA could then be purified and captured in a series of elutions. All nickel-purified elutions from standard transfections were tested for dIgA content via western blot.

Figure 12 shows elutions from batch *193 and that most IgA is present in elutions E1 to E6. SM, FT, and W represent starting material, flowthrough and wash respectively, while E1 to E11 represent elutions containing dIgA. Most IgA seems to be in dimeric form since bands are seen around 400kDa. Other bands seen at 560kDa could represent IgA in its tetrameric form. The bottom half of the image was removed since additional bands were only seen for starting material and flowthrough.

Commented [Ga38]: also describe the other bands

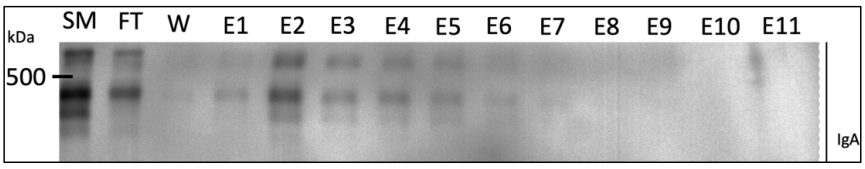

*Figure 12: Western blot for elutions from transfection batch *193*

Samples from the same elutions were subject to silver staining to assess their level of contamination by non-IgA proteins.

Figure 13 confirms that most IgA antibody is present between elutions E1 and E7. SM, FT and W represent starting material, flowthrough and wash respectively while E1 to E11 represent elutions containing dIgA. Most bands are seen at a height of 400kDa representing dimeric IgA. Additional bands seen at 150kDa and 300kDa suggest that elutions contain some impurities.

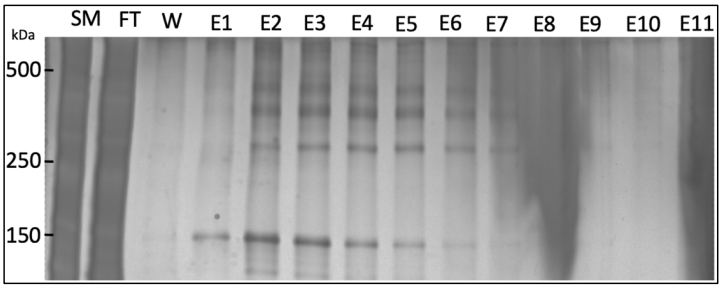

*Figure 13: Silver stain for elutions from transfection batch *193*

6.7. FPLC – AEX Chromatography

6.7.1. Fractionation curve from AEX in FPLC

The nickel purified elutions from batches containing dIgA were pooled for each batch. Pooled elutions from batch *189 and *191 were then combined as they were similarly pure in silver stain images. Running further purification steps two batches at a time maximise their efficiency. The combined *189 and *191 elutions were dialyzed in PBS (pH 7.4) to ensure that the start buffer is at least one pH unit above the pI of dIgA (5.7) so that IgA is negatively charged and binds the positively charged column. During gradient elution with NaCl, absorbance values were converted to a fractionation curve (Figure 14). This shows a main peak between elutions 10 and 22 with two shoulders around elution 25 and 29. The second and third peak are seen between elutions 35 to 42 and 43 to 46, respectively.

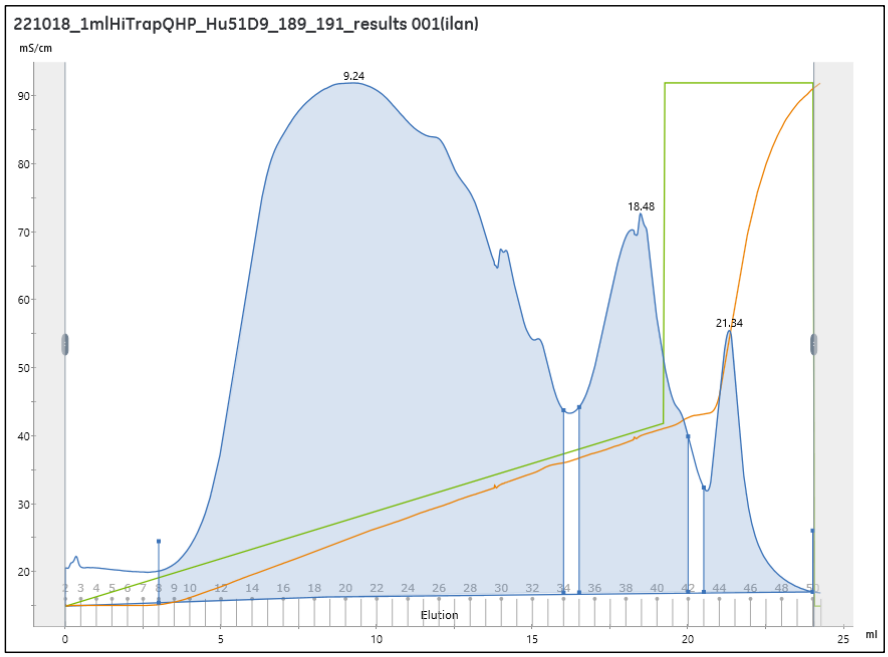

*Figure 14: Fractionation curve of AEX purified 51D9 from batches *189 and *191*

To test which elutions from AEX purification contain dIgA, a western blot with rabbit anti-IgA antibody was run using elutions 10 to 31 which represent the main peak in Figure 14 . *Figure 15* shows the starting material (SM), flowthrough (FT), wash (W) and elutions 10 to 31 with a molecular weight (kDa) ladder. The starting material shows a thick band around 400kDa. Most of the IgA is found in elutions 12 to 17 and mostly in dimeric form at 400 kDa.

Commented [GU39]: The way the blot on the right is exposed, it looks like most of it came out in the wash

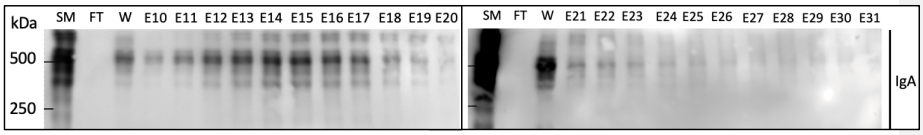

Figure 15: Western Blots of 22 elutions of 51D9 dIgA purified by AEX

6.7.2. Elution WB & Silver Stain

To validate the purity of AEX elutions, the silver stain images in Figure 16 show that elutions 12 to 17 contain not much other than dIgA with its dimeric form seen at 400kDa. Lane headers are the same as in Figure 15. The starting material shows a consistent smear throughout the lane suggesting a high impurity content. Elutions 21 to 27 show additional bands at 180kDa and 50kDa which could represent monomeric IgA and a contaminant protein, respectively. The stains seen around E12 and E13 as well as E17 and 19 represent impurities which occurred silver staining. In the laboratory, the gel bands could still be seen underneath, allowing for an assessment of AEX elution purity.

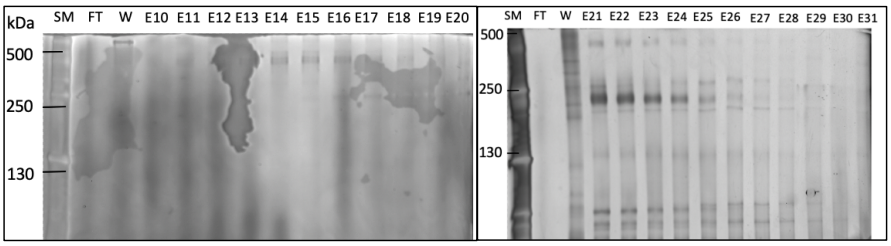

Figure 16: Silver Stain of 22 elutions of 51D9 dIgA purified by AEX

6.8. PNGase

6.8.1. PNG Western Blot

The PNGase enzyme had been used to show heavy glycosylation in purified IgA (unpublished). While this study could not identify which glycans were present, it highlighted the extent of IgA glycosylation. For this study, PNGase was used to aberrantly deglycosylate dIgA, in an attempt to elucidate if aberrant glycosylation could be achieved and how this might affect its ability to bind pIgR. This was done on another antibody (1F12) than the one used in transfection trials and transcytocis (51D9) since the latter had not yet been purified.

Purified samples were treated with PNGase for different amount of time to influence the level of degylcosylation.

Figure 17 shows a western blot image of 1F12 dIgA, control human dIgA and batch *120 supernatant treated with PNGase at 37°C for 4 hours in lanes 1 to 3 respectively. The same samples were loaded untreated as controls in lanes 5 to 7. The antibody used to visualize IgA was rabbit anti-human IgA. While the smear makes it difficult to decipher specific bands, IgA intensity decreases when treated with PNG. Lane 4 shows that no bands are visible when PNGase treated 1F12 dIgA is denatured at 100°C.

Commented [Ga40]: whith which antibody was the western blot performed?

Commented [Ga41]: PNG does not denature the sample, it deglycosylates the sample, thus there must be still a band seen in lane 4

Commented [Ga42]: the denaturation is due to the temperature and not due to PNG

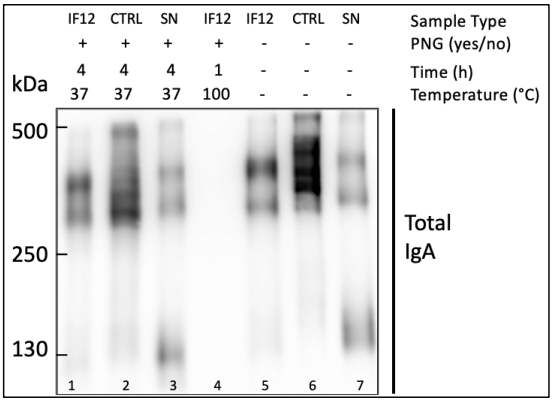

Figure 17: Western blot of dIgA and supernatant samples treated with PNG for 4 hours

To study the effect of incubation times on PNG treatment, samples from the first PNG trial were incubated with PNGase for 4, 6, 8 and 21 hours. Figure 18 shows 1F12 dIgA treated for 4, 6, 8 and 21 hours with PNG in lanes 1, 3, 5 and 7, respectively and without in lanes 2, 4, 6 and 8, respectively. It shows a gradual decrease in IgA signal intensity over time when PNGase is added to 1F12 dIgA during incubation. Human control dIgA treated for 6 and 21 hours with PNG is found in lane 9 and 11 and without PNG in lanes 10 to 12. Supernatant from batch *120 treated for 21 hours with PNG is found in lane 13 and without in lane 14. For control human dIgA and *120 supernatant, the opposite trend is seen where IgA intensity increases over time when PNGase is added.

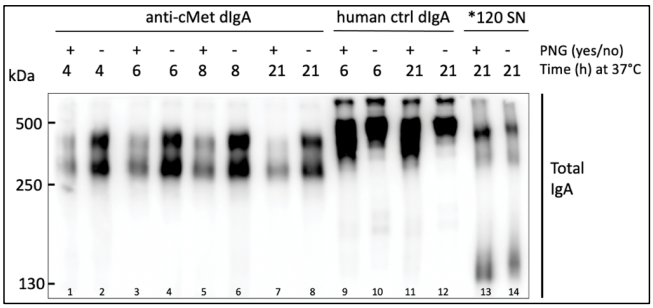

Figure 18: Western blot of dIgA and supernatant samples treated with PNG for 4 to 21 hours

6.9. Transcytocis

To characterize dIgA binding to pIgR, a key therapeutic function of dIgA in-vivo, a transcytocis assay was set up. The presence of dIgA was tested in apical well samples of transwells after applying it to the basolateral side. *Figure 19* shows a western blot of apical well samples following a transcytocis assay and visualised using rabbit anti-IgA antibody. For plain MDCK cells, lanes 2 and 3 show single bands around 300kDa, increasing in intensity between 48 and 72 hours. For MDCK 11 cells, lanes 6 to 9 show an additional band around 400kDa, increasing in intensity between 48 and 72 hours. No bands are seen for negative controls in lanes 5 and 10, while the positive control shows a thick band around 300kDa.

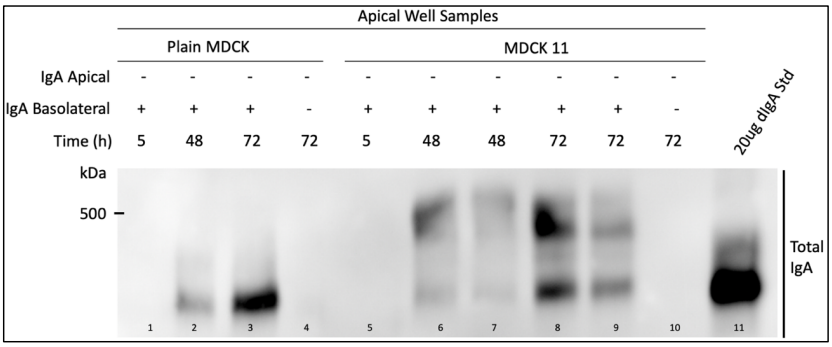

Figure 19: Western blot of standard transcytocis assay with 51D9 dIgA samples

Commented [Ga43]: you always have to state which antibody you have used for the western Blot

The transcytocis assay was modified to enhance dIgA-pIgR contact by placing the transwell insert directly onto a droplet of dIgA samples and leaving them incubating at 37°C during sampling. This was done in an attempt to reduce leaking and the incubation time after which dIgA could be seen. *Figure 20* shows an image of the western blot treated with anti-51D9 antibody. This shows no bands for samples in MCDK plain wells in lanes 2 to 7. For MDCK 11 wells, lanes 11 to 13 show a single band around 400kDa for 51D9 dIgA after 2,5 , 8 and 21 hours. Supernatant applied to MDCK11 wells shows 2 bands around 350 and 400kDa after 2,5 hours and none after 21 hours. The control for dIgA in lane 14 shows no bands while the control for supernatant in lane 15 shows a smear around 200kDa and 400kDa.

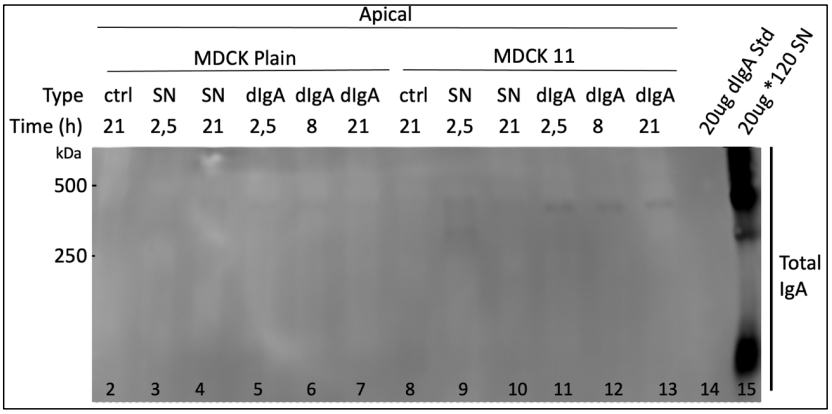

Figure 20: Western blot of droplet transcytocis assay for dIgA and supernatant samples

Commented [i44]: looks like gel

7. Discussion

7.1. Transfection

7.1.1. Standard batch growth rates

Cell growth and death were measured during dIgA expression as an indication of transfection efficiency and batch productivity. Thus transfection batches could be compared, and anomalies identified. One trend seen for all batches was considerable cell death in the first 24 hours post transfection, with an average of 71% dead cells in that timeframe. This implies that successfully transfected cells were limited from the beginning.

One hypothesis for this could be that cells are experiencing stress due to cytotoxicity of transfection reagents. Plasmid DNA is stored in TE Buffer, containing EDTA whose cytotoxic properties on human cells have been shown [53]. Exposing cells to EDTA buffer for 5 minutes might have reduced cell viability. A remedy for this could be to reduce exposure time of cells to plasmid DNA buffer by pre-diluting PEI and adding it right after DNA is added to the cells. Biological toxicity in plasmid samples was minimized by using purification kits specifying endotoxin levels below 1 EU/µg. By reusing plasmid DNA prep columns, endotoxins could have accumulated in the column and carried over to DNA samples, as they are known to have high affinities for hydrophobic lab equipment. As endotoxins can reduce transfection efficiencies, their presence in DNA samples could be tested before transfection by limulus amebocyte lysate assay (LAL), aiming for values below 0,5 endotoxin units/ml.

Another hypothesis for the observed cell death could be a planning error, which led to transfection reactions being performed with half the indicated HEK293 cell density. With fewer cells present, less cell-to-cell contact lowers the exchange of stimulation signals such as growth factors and therefore the chances to survive toxic transfection reagents [54]. In addition, the higher ratio of plasmid per cell means that DNA will be lost as cells divide, leading to lower transfection efficiencies. With cells recovering from cell death, it could explain why cells were growing exponentially at harvest, instead of reaching a plateau. In batch *196, where initial cell densities were correct, substantial cell death was also seen in suggesting that low cell densities are not the only cause for the observation of cell death.

7.1.2. Standard batch culture conditions

When comparing transfection culture conditions with key output parameters for standard batches, a few trends could be identified. Table 11 shows that transfection batches *190 and *194 had the lowest maximum cell densities during expression. With these batches also having the highest pre-transfection cell densities, high cell densities pre-transfection could have led to limited cell growth during expression. Several studies using HEK293 cells recommend transfecting when cells reach $1x10^6$ cells/ml [55]. Exceeding this density, risks that cells have stopped dividing at the point of transfection. While a lower cell density at the point of transfection would increase the required volume and the cost of maintenance media to get the same amount of cells, future trials could seek to optimize this trade-off.

When looking to correlate cell culture parameters with expression parameters, batch *191 is an anomaly as it shows high values in maximum cell density and growth rate but significantly lower estimated dIgA concentration. For all other batches, excluding batch *191, there is a positive correlation between maximum cell density and estimated dIgA concentration, with an R^2 value of 0,73. A possible explanation for this mismatch could be that transfection efficiency was low for batch *191, so that most cells responsible for the observed cell growth, were not expressing IgA and allocating energy to proliferation instead. Low plasmid quality, seen by high A260/A280 absorbance values for all samples in this batch, could explain poor transfection efficiency. To overcome this issue in future, successful transfections could be visualized by including a reporter gene such as green fluorescent protein into transfection plasmids. Transfection efficiency could be assessed by flow cytometry as transfected cells fluoresce and are separated [56].

When comparing western blot band intensities of cell supernatant and nickel-purified elutions a moderate correlation of R^2=0,54 was seen. This method could therefore be used as an indicator of batch productivity before purification. However, intensity measurements from western blot images are prone to error due to background and lane heterogeneity. Using concentrated cell supernatant to make this comparison could yield a stronger correlation since process impurities are minimized and western blot images would yield fewer and sharper bands.

An online design of experiments (DOE) identified biotic potential (rmax) as having the greatest effect on supernatant IgA band intensities and estimated concentration (xxx

7.1.3. Trial 1 results – small scale batch

Because of the implications media supplementation could have on dIgA process feasibility and glycosylation, yet the lack of studies to optimize this for dIgA, studying it was favoured over better established dIgA purification methods downstream. In the first trial, a variety of sugars, amino acids and acids were tested for their ability to promote cell growth and productivity. From Table 12, the condition F17+8mM asparagine showed highest values in maximum cell density, biotic potential, and band intensity, all significantly higher than the control. Supplementation of asparagine has been shown to reduce the amount of lactate in cells by shifting the metabolic pathway from lactate production to lactate consumption [57]. While cell metabolism was not analysed in this study, lower lactate levels could explain improved cell growth due to a reduction in intracellular acidification [58]. While the translatability remains limited for scale-down models, each condition in this trial was run with three replicates, offering initial insight into their effect on cell growth and productivity.

Commented [Ga45]: allgemeiner schreiben aber dennoch detaillierter

Commented [i46R45]: meinen sie fü diesen Teil "IgA production"?
der Gedanke war einen kurzen Text über die Produktion von IgA zu geben

Commented [Ga47]: es fehlt die Beschreibung wichtiger Begriffe die relevant für die Arbeit sind, z.B. Transcytose, pIgR usw..

Commented [i48R47]: danke, ich glaube jetzt sind die meisten beschrieben

7.1.4. Trial 2 results – medium scale batch

In the second trial, the promising condition of batch supplementation with 8mM asparagine was carried forward and scaled up along with the condition of F17 + 1% Tryptone N1. The promising trend of batch supplementation with 8mM asparagine still applies with Table 13 showing highest maximum cell densities, biotic potential, and exponential growth rates for that condition. It is notable that in the original study, of all those tested, asparagine was the only amino acid not showing enhanced accumulation in the medium when feeding with TN1 [56]. While they could not prove the effect of asparagine on boosting gene expression through single amino acid feeding, preliminary data from Trial 1 and 2 suggests a beneficial effect of asparagine supplementation on IgA production.

In previous studies, media supplementation with 1% Tryptone N1 has been linked to slight increased cell growth and substantial increases in protein synthesis [56]. From Table 13, the condition of F17 + 1% TN1 shows significantly lower cell growth in comparison to control with no additives. Albeit lower cell growth, this condition still yields highest IgA band intensities, which aligns with the hypothesis that peptones stimulate gene expression post transfection. A loss in dIgA band intensity between 135 and 168 HPT for condition TN1 suggests that maximum dIgA production is time dependent and could reduce expression times. The overall and time-sensitive effect on IgA expression warranted a further trial of scaling up the TN1 condition to standard transfection volumes.

7.1.5. Trial 2 results – medium scale fed batch

In the second part of Trial 2, fed-batch media supplementation with several sugars was tested four and six days post transfection. Previous studies had seen that IgA synthesis was promoted when cells were fed with glucose, galactose, and mannose, from lowest to greatest effect, respectively [57]. In Trial 2, an average 10% increase in dIgA band intensity was seen between samples taken at the point of feeding and two days after. The lack of significant changes might be because feeding concentrations were too low. This hypothesis is supported when looking at cell growth curves during expression for fed-batch conditions (Appendix H). There, only the F17 + 8mM Mannose condition shows the effect of feeding as cell growth rate increases right after the 96- and 140-hour feeding times. This could point to mannose being an optimal carbon source, readily entering glycolysis and the TCA cycle. In addition, its metabolism has been shown to be essential for dIgA synthesis [57].
A trend seen across all conditions for this trial, except for the condition of F17 + 8mM Glucose, is a loss of intensity of dIgA between 135 and 168 hours post transfection (Table 14). This could suggest that after 135 hours, glucose becomes a limiting substrate for the production of dIgA and without addition, dIgA starts to break down. Due to the lack of replicates, this observation requires validation and could warrant further investigation into glucose metabolism of HEK293F cells and its role in dIgA expression. Glucose measurements could be performed with an enzymatic coulometric method using a glucose oxidase kit.

7.1.6. Trial 3 results – standard scale batch

In Trial 3, batch supplementation with 1% Tryptone N1 was tested against a positive control with Freestyle (GlutaMAX) representing standard conditions. This was a scale up study following observations in Trial 2 which showed that F17 + 1% TN1 reduced cell death post transfection and increased estimated dIgA concentrations.

When comparing growth rates, it appears that for both conditions, exponential growth started 119 hours post transfection. Exponential growth rates differed however, with 2,37 in the control representing a 40% increase to 1,69 in TN1. This could be explained by the presence of a GlutaMAX supplement in the control, which has been optimized to improve cell growth by reducing toxic ammonia build-up through slower breakdown of L-Glutamine [78]. When planning this trial it was no included, to focus the use of reagents on comparison with standard conditions. Including a negative control of Freestyle F17 medium with no additives, could validate if GlutaMAX addition is causing increased exponential growth rates. A negative control could also show if TN1 addition too positively affects cell growth for dIgA expressing HEK293 cells, which could not be verified in comparison with GlutaMAX.

It is notable that for TN1 supplementation, cell death did not occur in the first 24 hours after transfection. The percentage of dead cells then followed a similar trend to viable cell density, rising exponentially at 119 hours post transfection and reaching a maximum of 10%. This differentiates it from the control condition in this trial as well as all other growth curves from standard transfection batches *189 to *195, where cell death rose rapidly in the first 24 hours post transfection and gradually decreased reaching an average of 22% dead cells at the point harvest. It suggests that TN1 displays anti-apoptotic properties during and/or after transfection. While some studies have suggested that peptones such as Tryptone may inhibit transfection, others have shown them to be anti-apoptotic [50] [59]. Observations in this trial seem to confirm the latter. Due to peptone's chemically undefined nature, the mechanism for this is poorly understood. Some proteomics studies have suggested that peptones downregulate proteins involved in cell cycle arrest thereby delaying apoptosis

[60]. Other studies suggest that peptones provide nutritional buffering, protecting cells during production cycles [61].

The notable difference in estimated dIgA concentration between the Freestyle (GlutaMAX) positive control and TN1 condition, with a of 13 fold increase in the latter seen in Table 15, demands further attention. The low values for dIgA concentration in the control seem anomalous. A hypothesis for this could be poor transfection efficiency with a similar reasoning to the anomaly seen with batch *191. Albeit an apparent lack of reliable control in this trial, 1% Tryptone N1 supplementation seems to promote dIgA expression. This is concurrent with observations from Trial 2 and therefore strengthens the hypothesis of peptones stimulating gene expression post transfection. This could be related to a higher amount of free amino acids present for IgA synthesis when peptones are broken down (Pham 2003). To integrate the use of TN1 into a standard process for dIgA expression, characterization of TN1 and its mechanisms is required. Further work could focus on identifying which Tryptone N1 components lead to reduced cell death and improved IgA expression, by individually supplementing amino acids and other known components.

Since the quantitative value of western blot band intensity measurements is limited, a general improvement for dIgA concentration measurements would be to use an ELISA assay. With this, IgA concentrations in supernatant can be measured by incubating HRP conjugated antibodies with samples in a 96 well plate. As they bind IgA's heavy chain, dIgA absorbance is measured and can be translated to concentration values using a standard curve. For completion of this work, purification of the TN1 supplemented batch is required to compare dIgA yields with standard conditions. The resulting dIgA's could then be tested for glycosylations using PNGase enzyme and receptor-binding using the transcytocis assay.

7.2. Anion Exchange Chromatography

7.2.1. Fraction elution graph

When comparing fractionation curve in Figure 14 with western blot of elutions in *Figure 15*, it seems that only the left shoulder of the peak is showing dIgA. This suggests that the main peak seen between elutions 10 and 32 contains another protein with a similar net charge as it was eluted at the same time. The silver stain from Figure 16 indicates that purified dIgA has been obtained, with most bands seen at 400kDa. Additional bands seen at 180kDa and 50kDa suggest some protein contamination in eluted samples. To avoid this in future, a cation exchange or size exclusion chromatography step could be included upstream of AEX to minimize impurity breakthrough while also enhancing viral clearance. To achieve better peak separation during fractionation, the linear elution gradient could be flattened by increasing elution times from 25 to 35 column volumes.

Meg's comments:

But was it at the same time? It came off the column in a separate peak aka slightly different times (which is what we want and what your results show happened!)

You could do another step of purification in the future like you suggested to get rid of the polymeric species for example. You'd probably want to use a size exclusion column though

7.3. PNGase

Treatment of purified dIgA with PNGase enzyme cleaved N-linked glycans to uncover and modify glycosylation profiles. dIgA samples treated with PNGase under varying time and temperature conditions were analysed by western blot and silver stain. These could not identify specific glycosylations due to an oversaturation of bands and lack of image sharpness. Western blot images in

Figure 17 seem to show, however, that 1F12 is heavily glycosylated with PNGase treated samples showing weaker band intensities. Overall, this suggests that PNGase can deglycosylate dIgA under non-denaturing conditions. Figure 18 shows that this effect is

Commented [GU49]: But was it at the same time? It came off the column in a separate peak aka slightly different times (which is what we want and what your results show happened!)

Commented [GU50R49]: You could do another step of purification in the future like you suggested to get rid of the polymeric species for example. You'd probably want to use a size exclusion column though

Commented [i51R49]: for the first comment:
I meant that the main peak which consists of elations 10 to 32 must contain another protein since dIgA was only seen in elutions 10 to 22 while the peak is still showing high absorbable and two bumps between elations 22 and 32

Commented [GU52R49]: Ok, I see. Maybe add a statement that explains the rest of the stuff you are talking about isn't visible on the SS (probably ran off the gel and was also removed during the final concetration step that uses a column with a MWCO of 100kDa)

time-dependent with PNGase treated dIgA samples showing a weakening of band intensities between 2 and 21 hours of incubation at 37°C.
It is notable that denaturing conditions of 100°C show no bands at all, as they should show individual chains that make up IgA. The variable and constant regions of IgG have been shown to denature at 61°C and 71°C respectively. Due to IgA being less stable than IgG, it is possible that denaturation occurs at lower temperatures and so that exposure to 100°C caused protein degradation. IgA denaturation could be achieved by increasing temperatures stepwise from 40°C upwards and testing for the presence of IgA chains via western blot.

As a next step, the function of dIgA treated with PNGase for 4 hours at 37°C, was tested in a transcytocis assay. This was done to see if aberrant glycosylation of dIgA affected pIgR binding and transcytocis. Studies have suggested that certain glycosylations such as sialyation are essential for transcytocis to occur (Paul, 2013). When looking at the western blot image of apical well samples, no significant difference in transcytocis could be seen between PNGase treated and untreated samples (Figure 28, Appendix I). This suggests that PNGase treatment of dIgA for 4 hours at 37°C does not affect dIgA's transcytocis abilities.

This experiment could be expanded by using PNGase treated dIgA samples with longer incubation times. Further experiments could analyse the glycosylation profile of purified dIgA from media supplementation trials. This could show how TN1 supplementation affects dIgA glycosylation and in doing so, characterize the structure of purified 51D9 dIgA. To improve glycoprofiling, lectins could be employed which bind glycans specifically. When coupled with HRP, their interaction with individual glycans could be visualized in western blots. A more precise approach would be to use lectin-microarray where dIgA molecules spotted onto a chip are glycoprofiled by incubating with biotinylated lectins and analysing N-glycan moieties by MALDI-MS. To extract dIgA molecules with specific glycosylations, lectin affinity chromatography could be used where lectins are bound to a column and select glycans based on lectin-binding site affinities. The resulting fractions, enriched for certain glycans, could be used to assess their impact on dIgA function or stability.

7.4. Transcytocis

7.4.1. Evaluation of standard transcytocis method

Several attempts of the transcytocis assay with the standard setup showed dIgA bands at 300kDa for MDCK plain and MDCK 11 wells (Figure 19). This suggests that dIgA must have leaked from the basolateral to the apical well, since MDCK plain cells do not express pIgR and cannot transcytose dIgA. Equally, MDCK 11 wells would only show a higher band since all dIgA transcytosed would have pIgR secretory component (SC) attached to them. Leaking may be due to the MDCK cell monolayer not having formed a full seal when the assay was started. The leak test used to assess confluence in this setup relies on visual identification of media levels having equalized, limiting its reliability. A more precise method would be to measure trans-epithelial electrical resistance (TEER) via two electrodes placed on the bottom of the transwell which detect small changes in impedance of current flow caused by tight junctions between cells. Leaking might have occurred during transcytocis due to the numerous samples being taken at several time intervals. These could have disturbed the cell layer through mechanical agitation or plate cooling, respectively.

Besides leaking, Figure 19 shows an additional band around 450kDa for MDCK 11 wells with increasing intensity over time. This is likely to represent dIgA with secretory component (sIgA) with a molecular weight around 400 to 500 kDa [63]. This suggests that while MDCK 11 cells also experienced leaking, some dIgA was transcytosed. Comparing band intensities for the bands seen at 400kDa with the standard 20µg dIgA band suggests that about 4µg were transcytosed, which represents 10% of the 40µg dIgA loaded into the basolateral well.

Commented [i53]: sc+dIgA is usually ~400-500kDa. SC alone is ~70kDa

7.4.2. Evaluation of droplet transcytocis method

An alternative method to the transcytocis assay was tested, whereby the transwell insert was placed onto a droplet containing dIgA samples. This was done in an effort to reduce leaking, assay times and amount of antibody required. Figure 20 shows that when using the droplet method, bands are only seen in MDCK11 wells. The supernatant sample in lane 9 shows two bands at 300kDa and 400kDa which likely represent dIgA and sIgA, respectively indicating that the well must have leaked since only sIgA is expected in apical wells. The bands seen at 400kDa for dIgA samples likely represent sIgA indicating that dIgA has bound

pIgR for transcytocis, and that no leaking occurred. As sIgA band intensity stayed the same over time, it suggests that dIgA did not accumulate in apical wells. The dIgA standard yielded no bands, which prevented verification of sIgA size shift and estimation of transcytocis efficiency. Nevertheless, this modification seems to have solved the leaking issue and reduced assay times with sIgA bands seen at 2,5 hours. Overall, these results show dIgA's ability to bind pIgR and undergo transcytosis, validating its key function in-vitro. With the droplet method proving transcytocis with fewer reagents than in the standard setup, it seems ideal to study the effect of PNGase treatment since less of the costly PNGase reagent would have to be used to treat dIgA samples beforehand.

Another way to assess transcytocis and purify sIgA would be to cut out the transwell filters on which MDCK cells have grown and vortex them in MEM medium. The resulting extract could then be immunoprecipitated by affinity chromatography where anti-SC antibodies bound to a protein G Sepharose column capture sIgA which can then be eluted. The presence of sIgA could then be visualized via western blot. Purified sIgA from this method could be used to test the effect of SC on dIgA's function and stability. For example through an antigen binding assay, where sIgA is added to a plate of CHO cells expressing IL13. After incubation and washing off unbound sIgA, addition of fluorescence-linked antibodies specific to SC and IL13 could enable immunofluorescent visualization of co-localization.

A characteristic which must be verified prior to dIgA's application in-vivo is its function blocking ability. This could be done by incubating dIgA with intramedullary collecting duct cells expressing IL13 and observing inhibition of STAT6 downstream.

8. Conclusion & Outlook

Commented [Ga54]: you have to discuss more your overall results and compare it with the literature; you are mainly discussing methods

The present work investigated how the production and in-vitro characterization of dIgA could be improved. The supplementation of transfection media looked to enhance HEK293 cell productivity while a transcytocis assay validated the ability of purified dIgA to bind pIgR.

The emergence of IgG immunoglobulins as promising therapeutics has led to the development of methods to produce them at scale. In contrast, while IgA has unique features for the treatment of autoimmune diseases such as ADPKD, studies to generate therapeutically relevant quantities are scarce. This is partly due to the difficulty of replicating their glycosylations and specialized conformation to target disease-markers. While the use of mammalian cells for IgA expression has addressed these challenges, low volumetric productivity remains a principal drawback. Supplementation of serum-media offers a promising solution to overcome this issue. While the cultivation of HEK293 cells in serum-free media is well-established, a cell-line specific feeding strategy for the expression of therapeutic IgA antibodies needs to be further optimised. This is done in consideration of IgA's glycoprofile due to the impact cultivation can have on effector functions.

In terms of dIgA expression, addition of Tryptone N1 (TN1) to serum-free media showed a 93% reduction in cell death post transfection and promoted dIgA expression in comparison to GlutaMAX. This highlights TN1's advantages for serum-free IgA production by optimizing the growth profile of HEK293 cells, a key aspect for biopharmaceutical production [53]. This study could not elucidate how media supplementation affects dIgA glycosylation. While this is not a critical aspect for preclinical trials, it remains of high interest for future studies due to characterize IgA's unique structure. Overall, this study provided an initial insight into the potential of peptone-supplementation to improve a HEK293 expression of dIgA.

In terms of pIgR binding, the ability of dIgA to bind pIgR and undergo transcytocis was confirmed. In addition to validating this therapeutic function, an alternative method was used which reduces the reagents and time needed to verify transcytocis. This method represents an effective tool to screen dIgA candidates for their key function.

Further work could test the beneficial effect of pIgR secretory component on the stability and binding abilities of dIgA through molecular target binding assays.

tion.

Commented [i55]: Consequently, a peptone-supplemented bioprocess needs to be optimized for a specific cell line or clone.
Davami 2015

9. Bibliography

Weimbs, T., Olsan, E. E., Matsushita, T. & Rezaei, M. (2015). Exploitation of the Polymeric Immunoglobulin Receptor for Antibody Targeting to Renal Cyst Lumens in Polycystic Kidney Disease. The Journal of biological chemistry, 290(25), 15679–15686. https://doi.org/10.1074/jbc.M114.607929

[1] PKD International, "pkdinternational.org," 2021. [Online]. Available: pkdinternational.org/what-is-pkd/adpkd/. [Accessed 3 January 2023].

[2] Olsan, E. E., Matsushita, T., Rezaei, M., & Weimbs, T. (2015). Exploitation of the Polymeric Immunoglobulin Receptor for Antibody Targeting to Renal Cyst Lumens in Polycystic Kidney Disease. *The Journal of biological chemistry*, *290*(25), 15679–15686. https://doi.org/10.1074/jbc.M114.607929

[3] Zhou, X., Davenport, E., Ouyang, J., Hoke, M. E., Garbinsky, D., Agarwal, I., Krasa, H. B., & Oberdhan, D. (2022). Pooled Data Analysis of the Long-Term Treatment Effects of Tolvaptan in ADPKD. *Kidney international reports*, *7*(5), 1037–1048. https://doi.org/10.1016/j.ekir.2022.02.009

[4] Torres, V. E., Chapman, A. B., Devuyst, O., Gansevoort, R. T., Perrone, R. D., Koch, G., Ouyang, J., McQuade, R. D., Blais, J. D., Czerwiec, F. S., Sergeyeva, O., & REPRISE Trial Investigators (2017). Tolvaptan in Later-Stage Autosomal Dominant Polycystic Kidney Disease. *The New England journal of medicine*, *377*(20), 1930–1942. https://doi.org/10.1056/NEJMoa1710030

[5] Torres, J. A., Kruger, S. L., Broderick, C., Amarlkhagva, T., Agrawal, S., Dodam, J. R., Mrµg, M., Lyons, L. A., & Weimbs, T. (2019). Ketosis Ameliorates Renal Cyst Growth in Polycystic Kidney Disease. *Cell metabolism*, *30*(6), 1007–1023.e5. https://doi.org/10.1016/j.cmet.2019.09.012

[6] Brüggemann, M., Williams, G. T., Bindon, C. I., Clark, M. R., Walker, M. R., Jefferis, R., Waldmann, H., & Neuberger, M. S. (1987). Comparison of the effector functions of human immunoglobulins using a matched set of chimeric antibodies. *The Journal of experimental medicine*, *166*(5), 1351–1361. https://doi.org/10.1084/jem.166.5.1351

[7] Lorin, V., & Mouquet, H. (2015). Efficient generation of human IgA monoclonal antibodies. *Journal of immunological methods*, *422*, 102–110. https://doi.org/10.1016/j.jim.2015.04.010

[8] Bergmann, C., Guay-Woodford, L. M., Harris, P. C., Horie, S., Peters, D. J. M., & Torres, V. E. (2018). Polycystic kidney disease. *Nature reviews. Disease primers*, *4*(1), 50. https://doi.org/10.1038/s41572-018-0047-y

[9] Al-Bhalal, L., & Akhtar, M. (2005). Molecular basis of autosomal dominant polycystic kidney disease. *Advances in anatomic pathology*, *12*(3), 126–133. https://doi.org/10.1097/01.pap.0000163959.29032.1f

[10] Yoder, B. K., Hou, X., & Guay-Woodford, L. M. (2002). The polycystic kidney disease proteins, polycystin-1, polycystin-2, polaris, and cystin, are co-localized in renal cilia. *Journal of the American Society of Nephrology : JASN*, *13*(10), 2508–2516. https://doi.org/10.1097/01.asn.0000029587.47950.25

[11] Dalagiorgou, G., Basdra, E. K., & Papavassiliou, A. G. (2010). Polycystin-1: function as a mechanosensor. *The international journal of biochemistry & cell biology*, *42*(10), 1610–1613. https://doi.org/10.1016/j.biocel.2010.06.017

[12] Brill, A. L., & Ehrlich, B. E. (2020). Polycystin 2: A calcium channel, channel partner, and regulator of calcium homeostasis in ADPKD. *Cellular signalling*, *66*, 109490. https://doi.org/10.1016/j.cellsig.2019.109490

[13] Winokurow, N., & Schumacher, S. (2019). A role for polycystin-1 and polycystin-2 in neural progenitor cell differentiation. *Cellular and molecular life sciences : CMLS*, *76*(14), 2851–2869. https://doi.org/10.1007/s00018-019-03072-x

[14] Xiao, Z., Zhang, S., Magenheimer, B. S., Luo, J., & Quarles, L. D. (2008). Polycystin-1 regulates skeletogenesis through stimulation of the osteoblast-specific transcription factor RUNX2-II. *The Journal of biological chemistry*, *283*(18), 12624–12634. https://doi.org/10.1074/jbc.M710407200

[15] Winyard, P., & Jenkins, D. (2011). Putative roles of cilia in polycystic kidney disease. *Biochimica et biophysica acta*, *1812*(10), 1256–1262. https://doi.org/10.1016/j.bbadis.2011.04.012

[16] Yamaguchi, T., Hempson, S. J., Reif, G. A., Hedge, A. M., & Wallace, D. P. (2006). Calcium restores a normal proliferation phenotype in human polycystic kidney disease epithelial cells. *Journal of the American Society of Nephrology : JASN*, *17*(1), 178–187. https://doi.org/10.1681/ASN.2005060645

[17] Wang, X., Wu, Y., Ward, C. J., Harris, P. C., & Torres, V. E. (2008). Vasopressin directly regulates cyst growth in polycystic kidney disease. *Journal of the American Society of Nephrology : JASN*, *19*(1), 102–108. https://doi.org/10.1681/ASN.2007060688

[18] Hopp, K., Hommerding, C. J., Wang, X., Ye, H., Harris, P. C., & Torres, V. E. (2015). Tolvaptan plus pasireotide shows enhanced efficacy in a PKD1 model. *Journal of the American Society of Nephrology : JASN*, *26*(1), 39–47. https://doi.org/10.1681/ASN.2013121312

[19] Sweeney, W. E., Chen, Y., Nakanishi, K., Frost, P., & Avner, E. D. (2000). Treatment of polycystic kidney disease with a novel tyrosine kinase inhibitor. *Kidney international*, *57*(1), 33–40. https://doi.org/10.1046/j.1523-1755.2000.00829.x

[20] Torres, V. E., Sweeney, W. E., Jr, Wang, X., Qian, Q., Harris, P. C., Frost, P., & Avner, E. D. (2004). Epidermal growth factor receptor tyrosine kinase inhibition is not protective in PCK rats. *Kidney international*, *66*(5), 1766–1773. https://doi.org/10.1111/j.1523-1755.2004.00952.x

[21] Holditch, S. J., Brown, C. N., Atwood, D. J., Lombardi, A. M., Nguyen, K. N., Toll, H. W., Hopp, K., & Edelstein, C. L. (2019). A study of sirolimus and mTOR kinase inhibitor in a hypomorphic *Pkd1* mouse model of autosomal dominant polycystic kidney disease. *American journal of physiology. Renal physiology*, *317*(1), F187–F196. https://doi.org/10.1152/ajprenal.00051.2019

[22] Takakura, A., Nelson, E. A., Haque, N., Humphreys, B. D., Zandi-Nejad, K., Frank, D. A., & Zhou, J. (2011). Pyrimethamine inhibits adult polycystic kidney disease by modulating STAT signaling pathways. *Human molecular genetics*, *20*(21), 4143–4154. https://doi.org/10.1093/hmg/ddr338

[23] Low, S. H., Vasanth, S., Larson, C. H., Mukherjee, S., Sharma, N., Kinter, M. T., Kane, M. E., Obara, T., & Weimbs, T. (2006). Polycystin-1, STAT6, and P100 function in a pathway that transduces ciliary mechanosensation and is activated in polycystic kidney disease. *Developmental cell*, *10*(1), 57–69. https://doi.org/10.1016/j.devcel.2005.12.005

[24] Olsan, E. E., Mukherjee, S., Wulkersdorfer, B., Shillingford, J. M., Giovannone, A. J., Todorov, G., Song, X., Pei, Y., & Weimbs, T. (2011). Signal transducer and activator of transcription-6 (STAT6) inhibition suppresses renal cyst growth in polycystic kidney disease. *Proceedings of the National Academy of Sciences of the United States of America*, *108*(44), 18067–18072. https://doi.org/10.1073/pnas.1111966108

[25] Johansen, F. E., & Brandtzaeg, P. (2004). Transcriptional regulation of the mucosal IgA system. *Trends in immunology*, *25*(3), 150–157. https://doi.org/10.1016/j.it.2004.01.001

[26] Monteiro, R. C., & Van De Winkel, J. G. (2003). IgA Fc receptors. *Annual review of immunology*, *21*, 177–204. https://doi.org/10.1146/annurev.immunol.21.120601.141011

[27] Butler J. E. (1998). Immunoglobulin diversity, B-cell and antibody repertoire development in large farm animals. *Revue scientifique et technique (International Office of Epizootics)*, *17*(1), 43–70. https://doi.org/10.20506/rst.17.1.1096

[28] Blutt, S. E., Miller, A. D., Salmon, S. L., Metzger, D. W., & Conner, M. E. (2012). IgA is important for clearance and critical for protection from rotavirus infection. *Mucosal immunology*, *5*(6), 712–719. https://doi.org/10.1038/mi.2012.51

[29] Jenny M. Woof, Marjolein van Egmond, Michael A. Kerr, Chapter 13 - Fc Receptors, Editor(s): Jiri Mestecky, Michael E. Lamm, Jerry R. McGhee, John Bienenstock, Lloyd Mayer, Warren Strober, Mucosal Immunology (Third Edition), Academic Press, 2005, Pages 251-265, ISBN 9780124915435, https://doi.org/10.1016/B978-012491543-5/50017-6.

[30] Woof, J. M., & Kerr, M. A. (2004). IgA function--variations on a theme. *Immunology*, *113*(2), 175–177. https://doi.org/10.1111/j.1365-2567.2004.01958.x

[31] Dechant, M., & Valerius, T. (2001). IgA antibodies for cancer therapy. *Critical reviews in oncology/hematology*, *39*(1-2), 69–77. https://doi.org/10.1016/s1040-8428(01)00105-6

[32] Hart, F., Danielczyk, A., & Goletz, S. (2017). Human Cell Line-Derived Monoclonal IgA Antibodies for Cancer Immunotherapy. *Bioengineering (Basel, Switzerland)*, *4*(2), 42. https://doi.org/10.3390/bioengineering4020042

[33] Taylor, A. K., & Wall, R. (1988). Selective removal of alpha heavy-chain glycosylation sites causes immunoglobulin A degradation and reduced secretion. *Molecular and cellular biology*, *8*(10), 4197–4203. https://doi.org/10.1128/mcb.8.10.4197-4203.1988

[34] Maurer, M. A., Meyer, L., Bianchi, M., Turner, H. L., Le, N. P. L., Steck, M., Wyrzucki, A., Orlowski, V., Ward, A. B., Crispin, M., & Hangartner, L. (2018). Glycosylation of Human IgA Directly Inhibits Influenza A and Other Sialic-Acid-Binding Viruses. *Cell reports*, *23*(1), 90–99. https://doi.org/10.1016/j.celrep.2018.03.027

[35] Brunke, C., Lohse, S., Derer, S., Peipp, M., Boross, P., Kellner, C., Beyer, T., Dechant, M., Royle, L., Liew, L. P., Leusen, J. H., & Valerius, T. (2013). Effect of a tail piece cysteine deletion on biochemical and functional properties of an epidermal growth factor receptor-directed IgA2m(1) antibody. *mAbs*, *5*(6), 936–945. https://doi.org/10.4161/mabs.26396

[36] Kerr, M. A., Senior, B. W., & Loomes, L. M. (1991). Microbial IgA proteases and virulence. *Reviews in Medical Microbiology, 2*(2), 200-207.

[37] Beyer, T., Lohse, S., Berger, S., Peipp, M., Valerius, T., & Dechant, M. (2009). Serum-free production and purification of chimeric IgA antibodies. *Journal of immunological methods*, *346*(1-2), 26–37. https://doi.org/10.1016/j.jim.2009.05.002

[38] Bastian, A., Kratzin, H., Eckart, K., & Hilschmann, N. (1992). Intra- and interchain disulfide bridges of the human J chain in secretory immunoglobulin A. *Biological chemistry Hoppe-Seyler*, *373*(12), 1255–1263. https://doi.org/10.1515/bchm3.1992.373.2.1255

[39] Roos, A., Bouwman, L. H., van Gijlswijk-Janssen, D. J., Faber-Krol, M. C., Stahl, G. L., & Daha, M. R. (2001). Human IgA activates the complement system via the mannan-binding lectin pathway. *Journal of immunology (Baltimore, Md. : 1950)*, *167*(5), 2861–2868. https://doi.org/10.4049/jimmunol.167.5.2861

[40] Olsan, E. E., Mukherjee, S., Wulkersdorfer, B., Shillingford, J. M., Giovannone, A. J., Todorov, G., Song, X., Pei, Y., & Weimbs, T. (2011). Signal transducer and activator of transcription-6 (STAT6) inhibition suppresses renal cyst growth in polycystic kidney disease. *Proceedings of the National Academy of Sciences of the United States of America*, *108*(44), 18067–18072. https://doi.org/10.1073/pnas.1111966108

[41] Turula, H., & Wobus, C. E. (2018). The Role of the Polymeric Immunoglobulin Receptor and Secretory Immunoglobulins during Mucosal Infection and Immunity. *Viruses*, *10*(5), 237. https://doi.org/10.3390/v10050237

[42] Low, S. H., Vasanth, S., Larson, C. H., Mukherjee, S., Sharma, N., Kinter, M. T., Kane, M. E., Obara, T., & Weimbs, T. (2006). Polycystin-1, STAT6, and P100 function in a pathway that transduces ciliary mechanosensation and is activated in polycystic kidney disease. *Developmental cell*, *10*(1), 57–69. https://doi.org/10.1016/j.devcel.2005.12.005

[43] Darvish, M., Behdani, M., Shokrgozar, M. A., Pooshang-Bagheri, K., Shahbazzadeh, D., (2015). Development of protective agent against Hottentotta saulcyi venom using camelid single-domain antibody. *Molecular Immunology*, *68*(2), 412-420. https://doi.org/10.1016/j.molimm.2015.10.002.

[44] Davami, F., Eghbalpour, F., Nematollahi, L., Barkhordari, F., & Mahboudi, F. (2015). Effects of Peptone Supplementation in Different Culture Media on Growth, Metabolic Pathway and Productivity of CHO DG44 Cells; a New Insight into Amino Acid Profiles. *Iranian biomedical journal*, *19*(4), 194–205. https://doi.org/10.7508/ibj.2015.04.002

[45] Lohse, S., Derer, S., Beyer, T., Klausz, K., Peipp, M., Leusen, J. H., van de Winkel, J. G., Dechant, M., & Valerius, T. (2011). Recombinant dimeric IgA antibodies against the epidermal growth factor receptor mediate effective tumor cell killing. *Journal of immunology (Baltimore, Md. : 1950)*, *186*(6), 3770–3778. https://doi.org/10.4049/jimmunol.1003082

[46] Lorin, V., & Mouquet, H. (2015). Efficient generation of human IgA monoclonal antibodies. *Journal of immunological methods*, *422*, 102–110. https://doi.org/10.1016/j.jim.2015.04.010

[47] Hossler, P., Khattak, S. F., & Li, Z. J. (2009). Optimal and consistent protein glycosylation in mammalian cell culture. *Glycobiology*, *19*(9), 936–949. https://doi.org/10.1093/glycob/cwp079

[48] Qiagen. (n.d.). Key steps in plasmid purification protocols. Retrieved January 8, 2023, from https://www.qiagen.com/us/knowledge-and-support/knowledge-hub/technology-and-research/plasmid-resource-center/key-steps-in-plasmid-purification-protocols

[49] Beyer, T., Lohse, S., Berger, S., Peipp, M., Valerius, T., & Dechant, M. (2009). Serum-free production and purification of chimeric IgA antibodies. *Journal of immunological methods*, *346*(1-2), 26–37. https://doi.org/10.1016/j.jim.2009.05.002

[50] Schlaeger E. J. (1996). The protein hydrolysate, Primatone RL, is a cost-effective multiple growth promoter of mammalian cell culture in serum-containing and serum-free media and displays anti-apoptosis properties. *Journal of immunological methods*, *194*(2), 191–199. https://doi.org/10.1016/0022-1759(96)00080-4

[51] Pham, P. L., Perret, S., Cass, B., Carpentier, E., St-Laurent, G., Bisson, L., Kamen, A., & Durocher, Y. (2005). Transient gene expression in HEK293 cells: peptone addition posttransfection improves recombinant protein synthesis. *Biotechnology and bioengineering*, *90*(3), 332–344. https://doi.org/10.1002/bit.20428

[52] McLenachan, S., Sarsero, J. P., & Ioannou, P. A. (2007). Flow-cytometric analysis of mouse embryonic stem cell lipofection using small and large DNA constructs. *Genomics*, *89*(6), 708–720. https://doi.org/10.1016/j.ygeno.2007.02.006

[53] Ogundele M. O. (1999). Cytotoxicity of EDTA used in biological samples: effect on some human breast-milk studies. *Journal of applied toxicology : JAT*, *19*(6), 395–400. https://doi.org/10.1002/(sici)1099-1263(199911/12)19:6<395::aid-jat590>3.0.co;2-5

[54] Thermo Fisher. (n.d.). *Factors influencing transfection efficiency*. Retrieved January 15, 2023, from https://www.thermofisher.com/at/en/home/references/gibco-cell-culture-basics/transfection-basics/factors-influencing-transfection-efficiency.html

[55] Liste-Calleja, L., Lecina, M., & Cairó, J. J. (2014). HEK293 cell culture media study towards bioprocess optimization: Animal derived component free and animal derived component containing platforms. *Journal of bioscience and bioengineering*, *117*(4), 471–477. https://doi.org/10.1016/j.jbiosc.2013.09.014

[56] Pham, P. L., Perret, S., Cass, B., Carpentier, E., St-Laurent, G., Bisson, L., Kamen, A., & Durocher, Y. (2005). Transient gene expression in HEK293 cells: peptone addition posttransfection improves recombinant protein synthesis. *Biotechnology and bioengineering*, *90*(3), 332–344. https://doi.org/10.1002/bit.20428

[57] Pažitná, L., Nemčovič, M., Pakanová, Z., Baráth, P., Aliev, T., Dolgikh, D., Argentova, V., & Katrlík, J. (2020). Influence of media composition on recombinant monoclonal IgA1 glycosylation analysed by lectin-based protein microarray and MALDI-MS. *Journal of biotechnology*, *314-315*, 34–40. https://doi.org/10.1016/j.jbiotec.2020.03.009

[58] Cruz, H. J., Freitas, C. M., Alves, P. M., Moreira, J. L., & Carrondo, M. J. (2000). Effects of ammonia and lactate on growth, metabolism, and productivity of BHK cells. *Enzyme and microbial technology*, *27*(1-2), 43–52. https://doi.org/10.1016/s0141-0229(00)00151-4

[59] Davami, F., Baldi, L., Rajendra, Y., & M Wurm, F. (2014). Peptone Supplementation of Culture Medium Has Variable Effects on the Productivity of CHO Cells. *International journal of molecular and cellular medicine*, *3*(3), 146–156.

[60] Kim, J. Y., Kim, Y. G., Han, Y. K., Choi, H. S., Kim, Y. H., & Lee, G. M. (2011). Proteomic understanding of intracellular responses of recombinant Chinese hamster ovary cells cultivated in serum-free medium supplemented with hydrolysates. Applied microbiology and biotechnology, 89(6), 1917–1928. https://doi.org/10.1007/s00253-011-3106-9

[61] Brooks, J., Sengupta, N., & Holdread, S. (2021, August 9). *Peptones: Over 100 years of life-saving innovation*. Chemistry World. Retrieved January 4, 2023, from https://www.chemistryworld.com/eureka-moments/peptones-over-100-years-of-life-saving-innovation/4014055.article

[62] Rochereau, N., Drocourt, D., Perouzel, E., Pavot, V., Redelinghuys, P., Brown, G. D., Tiraby, G., Roblin, X., Verrier, B., Genin, C., Corthésy, B., & Paµl, S. (2013). Dectin-1 is essential for reverse transcytosis of glycosylated SIgA-antigen complexes by intestinal M cells. *PLoS biology*, *11*(9), e1001658. https://doi.org/10.1371/journal.pbio.1001658

[63] Woof, J. M., & Russell, M. W. (2011). Structure and function relationships in IgA. *Mucosal immunology*, *4*(6), 590–597. https://doi.org/10.1038/mi.2011.39

[64] Tan, Y. C., Blumenfeld, J., & Rennert, H. (2011). Autosomal dominant polycystic kidney disease: genetics, mutations and microRNAs. *Biochimica et biophysica acta*, *1812*(10), 1202–1212. https://doi.org/10.1016/j.bbadis.2011.03.00

[65] Virdi, V., Juarez, P., Boudolf, V., & Depicker, A. (2016). Recombinant IgA production for mucosal passive immunization, advancing beyond the hurdles. *Cellular and molecular life sciences : CMLS*, *73*(3), 535–545. https://doi.org/10.1007/s00018-015-2074-0

[66] Weimbs, T., Shillingford, J. M., Torres, J., Kruger, S. L., & Bourgeois, B. C. (2018). Emerging targeted strategies for the treatment of autosomal dominant polycystic kidney disease. *Clinical kidney journal*, *11*(Suppl 1), i27–i38. https://doi.org/10.1093/ckj/sfy089

[67] Hosting, A. (2020, May 7). *What is tangential flow filtration (TFF) and where is it used? TBL Plastic. Retrieved February 3, 2023. from* https://tblplastics.com/tangential-flow-filtration-tff/

[68]

Ye, D., Dawson, K. A., & Lynch, I. (2015). A TEM protocol for quality assurance of in vitro cellular barrier models and its application to the assessment of nanoparticle transport mechanisms across barriers. *The Analyst*, *140*(1), 83–97. https://doi.org/10.1039/c4an01276c

[69] Lombana, 2019 https://doi.org/10.1080/19420862.2019.1622940

[70 Rocherau, 2013 doi:10.1371/journal.pbio.1001658

[71] Mazanec MB, Kaetzel CS, Lamm ME, Fletcher D, Nedrud JG: Intracellular neutralization of virus by immunoglobulin A antibodies. Proc Natl Acad Sci USA 89:6901–6905, 1992

[74]

https://doi.org/10.1074/jbc.M210665200

[72] EMA. (1999). ICH topic Q6B specifications: Test procedures and acceptance criteria for biotechnological/biological products. European Medicines Agency.

Villacrés, 2021

Villacrés, C., Tayi, V. S., & Butler, M. (2021). Strategic feeding of NS0 and CHO cell cultures to control glycan profiles and immunogenic epitopes of monoclonal antibodies. Journal of Biotechnology, 333, 49–62. https://doi.org/10.1016/j.jbiotec.2021.04.005

[78]

https://www.thermofisher.com/at/en/home/life-science/cell-culture/mammalian-cell-culture/media-supplements/glutamax-media.html

10. List of Figures

11. List of Tables

12. List of Abbreviations

Abbreviation	Meaning
ADCC	Antibody dependent cell toxicity
ADPKD	Adult Dominant Polycystic Kidney Disease
AEX	Anion Exchnage Chromaography
ARPKD	Adult Recessive Polycystic Kidney Disease
BSA	Bovine Serum Albumin
Ca^{2+}	Calcium
cAMP	Cyclic adenosine monophosphate
CHO	Chinese Hamster Ovary
DC%	Dead Cell Percentage
DI	Diionized
dIgA	Dimeric immunoglobulin A
DMSO)	Dimethyl sulfoxide
DNA	Deoxyribonucleic acid
DOE	Design of experiments
DTA	Droplet transcytocis assay
DTT	**D**ithiothreitol
EB	Elution buffer for Nickel Chromatography
EDTA	Ethylenediaminetetraacetic acid
EGFR	Epidermal growth factor receptor
EqB	Equilibration buffer for Nickel Chromatography
ER	Endoplasmic Reticulum
ERK/MAPK	Mitogen-activated protein kinase
FcαRI	Fragment crystallising α receptor I
FPLC	Fast protein liquid chromatography
H_2O	Water
HEK	Human embryo kidney
His-tag	Histidine residues
HPT	Hours post transfection
HRP	Horseraddish peroxidase
IEX	Ion exchange chromatography
IL-13	Interleukin 13
IP	**I**mmunoprecipitation
kDa	Kilo Daltons
LAL	**L**imulus amebocyte lysate assay
LB)	Luria-Bertani
LDL	Low-density lipoprotein
LED	Light emitting diode
MALDI-MS	Matrix-assisted laser desorption/ionization – Mass Spectrometry
MDCK	Mandin Darby Canine Kidney
MDCK	Mandin Darby Canini Kidney
MEM	Minimum essential medium
mTOR	Mammalian target of rapamycin
N_2	Nitrogen

Abbreviation	Meaning
NaCl	Sodium Chloride
NaOH	Sodium hydroxide
Ni^{2+}	Nickel
PBS	Phosphate-buffered Saline
PC1	Polycystin 1
PC2	Polycystin 2
PEI	Polyethylenimine
pen/strep	Penecillin/Streptomycin
pH	Potential of hydrogen
PI	Protease inhibitor
pI	Isoelectric point
pIgR	Polymeric immunoglobulin receptor
PKD	Polycystic Kidney Disease
PMSF	Phenylmethylsulfonyl fluoride
PNGase	Peptide:N-glycosidase
PVDF	Polyvinylidene fluoride
rmax	Biotic potential
SC	Secretory Component
SD	Standard Deviation
SdIgA	Secretory dimeric immunoglobulin A
SDS PAGE),	Sodium dodecyl sulfate–polyacrylamide gel electrophoresis
SM	Small molecule
STAT3	Signal transducer and activator of transcription 3
STAT6	Signal transducer and activator of transcription 6
TBST	Tris-Buffered Saline + Tween
TE	Tris-EDTA
TEER	Trans-epithelial electrical resistance
TG	Tris-Glycine
TGS	Tris-Glycine-SDS
TN1	Tryptone N1
UV	Ultraviolet
V2R	Vasopressin 2 receptor
VCD	Viable Cell Density
WB	Wash Buffer for Nickel Chromatography

13. Appendix

13.1. Appendix A

Table 16: Equations used to calculate output parameters

Name and Units of Parameter	Equation	Meaning of components
Population doubling time (days)	log(N2/N1) / log(2)	N2: cell count at harvest; N1: cell count at transfection
Biotic potential (cells/day/cell)	$e^{\ln(N2/N1) \ / \ (t2 - t1)}$	N2: cell count at start of exponential growth; N1: cell count at end of exponential growth; t2: days post transfection at start of exponential growth; t1: days post transfection at end exponential growth;
IgA concentration (µg/µl)	y/m – c	y: WB band intensity; m: slope of standard dilution curve; c: residual of standard dilution curve
Cell viability (cells/ml)	N/4 x 20.000	N: number of viable cells counted on 4 squares of hemacytometer

13.2. Appendix B

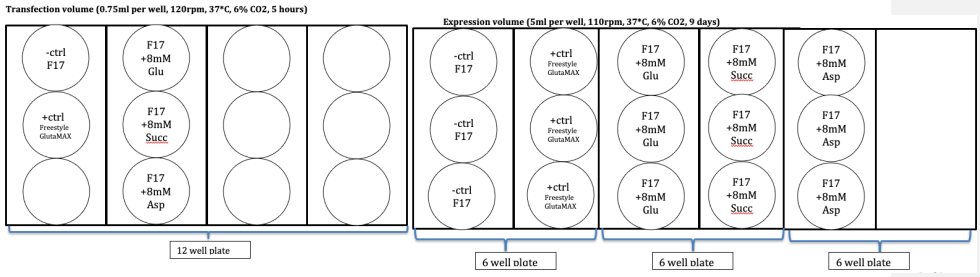

Figure 21: Setup of Transfection and Expression for Trial 1

13.3. Appendix C

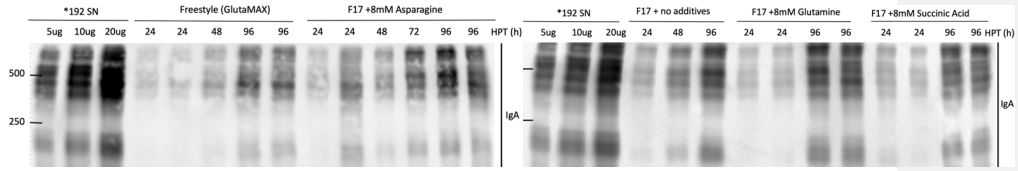

Figure 22: Western blot of Trial 1 supernatant samples (Antibody: anti-human IgA)

13.4. Appendix D

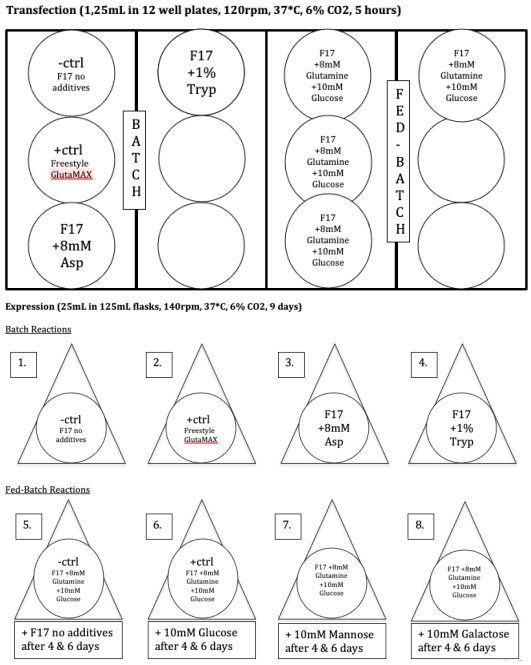

Figure 23: Setup of Transfection and Expression for Trial 2

13.5. Appendix E

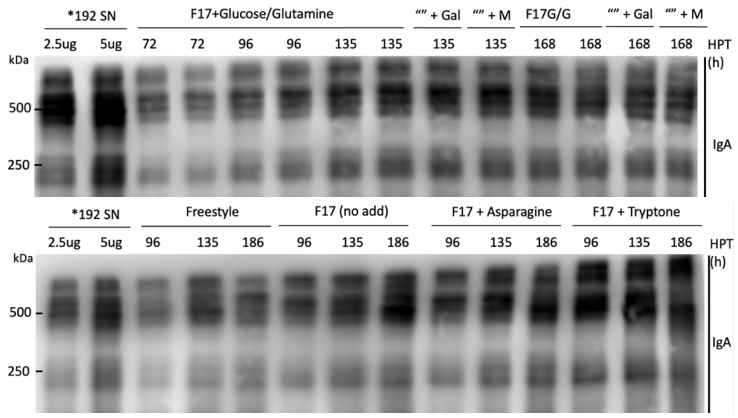

Figure 24: Western blot of Trial 2 supernatant samples (antibody: anti-human IgA)

13.6. Appendix F

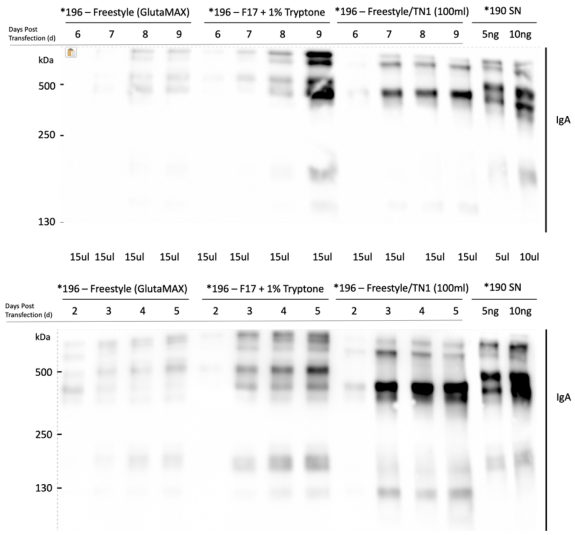

Figure 25: Western blot of Trial 3 supernatant samples (antibody: anti-human IgA)

13.7. Appendix G

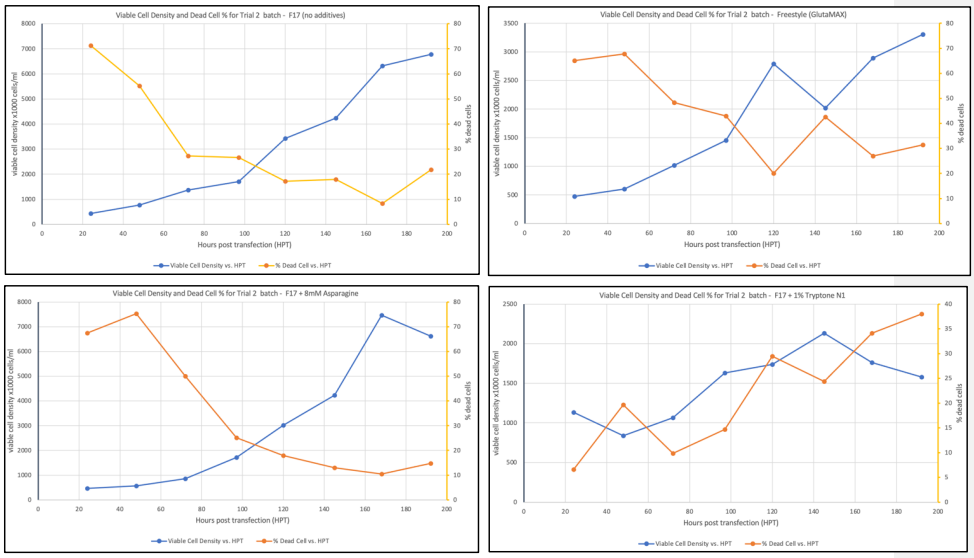

Figure 26: Growth Curves for Trial 2 - batch

13.8. Appendix H

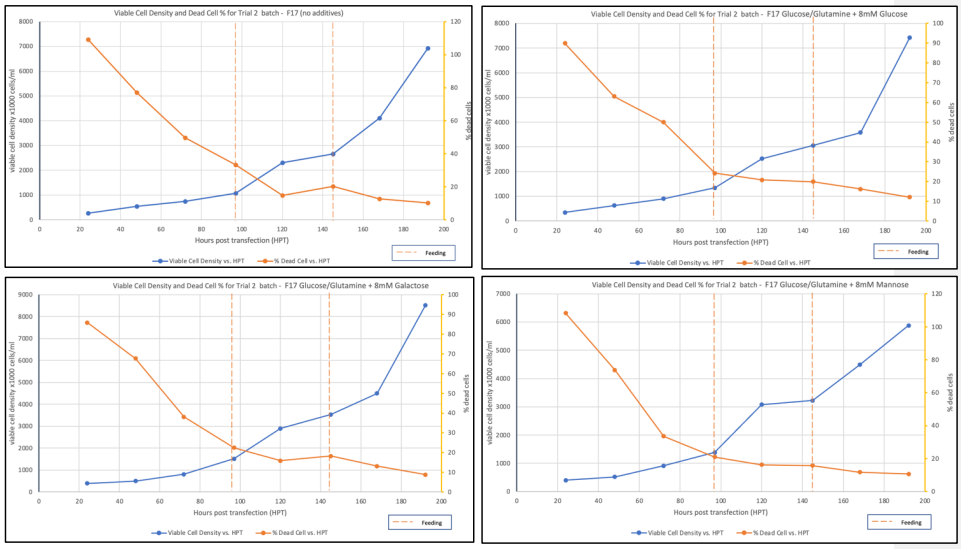

Figure 27: Growth Curves for Trial 2 - fed-batch

13.9. Appendix I

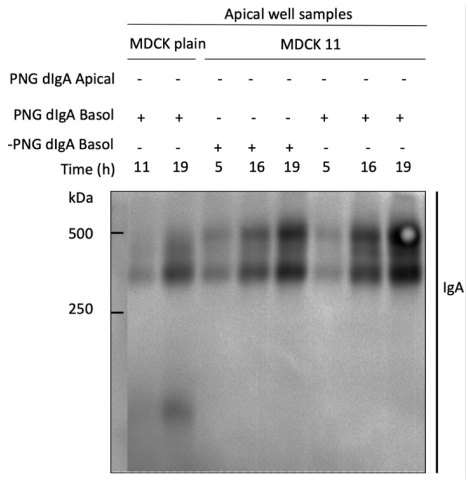

Figure 28: Western blot of transcytocis with PNG samples (antibody: rabbit anti-human IgA)